AREVA Calculation #32-9200249-000, "Diablo Canyon Power Plant Unit 2 Pzr Safety and Spray Nozzles Planar Flaw Analysis - Non Proprietary"

AREVA

CALCULATION SUMMARY SHEET (CSS)

Document No. 32 - 9200249 - 000 Safety Related: ☒ Yes ☐ No

Title Diablo Canyon Power Plant Unit 2 PZR Safety and Spray Nozzles Planar Flaw Analysis – Non Proprietary

PURPOSE AND SUMMARY OF RESULTS:

AREVA NP Inc. proprietary information in the document are removed and their locations are indicated by pairs of braces "[ ]". This document is the non-proprietary version of AREVA Document 32-9199805-000.

Purpose

The purpose of this document is to analyze the acceptability of indications detected or assumed to exist based on the results of the 2013 seventeenth refueling outage (2R17) inservice inspection that are considered rejectable in the overlaid Pressurizer (PZR) Safety and Spray Nozzles of Diablo Canyon Power Plant (DCPP) Unit 2. The reported rejectable indications are evaluated per the ASME B&PV Code Section XI, IWB-3514. In addition, the planar indications or the occluded zones requiring postulation of planar flaws are evaluated per ASME B&PV Code Section XI, IWB-3600.

Summary and Conclusion

This document performed flaw evaluations for indications found in DCPP Unit 2 PZR Safety Nozzles A, and NDE occlusion zones in PZR Safety Nozzles B and C and PZR Spray Nozzle. The conclusion of the flaw evaluations show that the indications in PZR Safety Nozzle A and NDE occlusion regions in PZR Safety Nozzles B and C and PZR Spray Nozzle meet the flaw acceptance standards of ASME B&PV Code Section XI, IWB-3514. All indications and postulated flaws in the NDE occlusion zones for all nozzles meet the ASME B&PV Code Section XI,IWB-3640.

THE FOLLOWING COMPUTER CODES HAVE BEEN USED IN THIS DOCUMENT:

CODE/VERSION/REV	CODE/VERSION/REV
AREVACGC 5.0	

THE DOCUMENT CONTAINS ASSUMPTIONS THAT SHALL BE VERIFIED PRIOR TO USE

☐ YES
☒ NO

Review Method: ☒ Design Review (Detailed Check)
☐ Alternate Calculation

Signature Block

Name and Title (printed or typed)	Signature	P/R/A and LP/LR	Date	Pages/Sections Prepared/Reviewed/Approved
Samer H Mahmoud Principal Engineer	S H	P	3-5-13	All
Silvester J Noronha Engineer IV	S J Noronha	R	3/5/13	All
Tim M Wiger Unit Manager	T.M. Wiger	A	3/5/13	All

Note: P/R/A designates Preparer (P), Reviewer (R), Approver (A);
LP/LR designates Lead Preparer (LP), Lead Reviewer (LR)

Project Manager Approval of Customer References (N/A if not applicable)

Name (printed or typed)	Title (printed or typed)	Signature	Date
N/A			

Mentoring Information (not required per 0402-01)

Name (printed or typed)	Title (printed or typed)	Mentor to: (P/R)	Signature	Date
N/A				
N/A				

Record of Revision

Revision No.	Pages/Sections/Paragraphs Changed	Brief Description / Change Authorization
000	All	Original Release

Table of Contents

Table of Contents
(continued)

Table of Contents
(continued)

List of Tables

List of Tables
(continued)

List of Figures

1.0 INTRODUCTION

An inservice inspection of Diablo Canyon Power Plant (DCPP) Unit 2 overlaid Pressurizer (PZR) Safety and Spray nozzles revealed the existence of rejectable indications in Safety Nozzle A. In PZR Safety Nozzles B and C and Spray Nozzle, an occlusion zone, where lack of non-destructive examination (NDE) coverage, was observed. The indications and occlusion areas are described in the Diablo Canyon Power Plant Design Input Transmittal (DIT) summarized in References [1]. Disposition of all reported laminar indications per the rules of the acceptance standards of ASME B&PV Code Section XI [2] are reported in Reference [3].

A majority of the indications (primarily laminar) were observed in the PZR safety and spray nozzles within the low alloy steel nozzles near the shoulder region of these nozzles. In safety nozzle A, where two indications are observed in the shoulder region, a planar flaw of 0.080-inches depth into the weld overlay is conservatively assumed. In safety nozzle C, acceptable laminar indications of 2-inches or less are observed in the middle of the weld overlay above the stainless steel safe-end and weld. In addition, postulated planar flaws are evaluated in the occluded zones under these laminar indications. The reported rejectable indications are evaluated per the ASME B&PV Code Section XI, IWB-3514. In addition, the planar indications or the occluded zones requiring postulation of planar flaws are evaluated per ASME B&PV Code Section XI, IWB-3600.

This document makes use of the rules in the Appendix C of ASME B&PV Code Section XI [2] to analyze the indications for the remainder of the plants life. All design input pertinent to completing the analysis of these indications is derived from the original documents, which were used to qualify the original designs of the safety and spray nozzle overlay. The original FSWOL design calculations involved sizing calculations [4,5], structural evaluation [6, 19], weld residual stress analysis [7, 17] and fracture mechanics analysis [9, 9]. The fracture mechanics analyses involved analyzing postulated ID-surface connected flaws that extend through 75% of the original nozzle thickness. The recent inservice inspection detected indications are much smaller than the flaws postulated during the original fracture mechanics qualification of the FSWOL design. Also, the indications are all embedded within the body of the nozzle and overlay; therefore, no primary water stress corrosion crack growth mechanism would occur. The only mechanism by which indications could grow is fatigue crack growth.

This document provides a description of the indications, postulated flaws, applicable fatigue crack growth laws, fatigue crack growth analysis, and finally the predicted final flaw sizes are evaluated in accordance with the rules of ASME B&PV Code Section XI, IWB-3600.

2.0 ANALYTICAL METHODOLOGY

This analysis postulates both circumferential and axial sub-surface flaws which may propagate by fatigue crack growth through the body of the safety nozzles and FSWOL, governed by crack growth rates and applied stress intensity factor. It is noted that the original fracture mechanics qualification of the FSWOL design, which was performed in 2007, used 38 year of remaining service life. The current analysis will be performed maintaining the 38 year of remaining service life. Fatigue crack growth analysis will be performed for 38 years of service life. Applied stresses include both transient and sustained normal operating loads. The analysis will determine the total amount of fatigue crack growth in 38 years. The predicted final flaw sizes are evaluated in accordance with the rules of ASME B&PV Code Section XI, IWB-3600.

2.1 Indications Shapes and Locations

Based on the Design Input Transmittal (DIT), References [1], the results of the PZR safety and spray nozzles inspection are summarized below.

2.1.1 PZR Safety Nozzle A Inspection

PZR Safety Nozzle A inspection detected 5 laminar flaw indications. The disposition of PZR Safety Nozzle A laminar flaws in accordance with the rules of ASME B&PV Code Section XI, IWA-3360 and IWB-3514 is provided in Reference [3]. Two of the indications in PZR Safety Nozzle A (indications 1 and 1A) are measured to be 0.08 inch deep through the thickness and 16.3 inches long around the circumference. Indications 1 and 1A are located within the FSWOL volume with the first tip located at the interface between the FSWOL and the low alloy steel nozzle and the second tip extends 0.08 radially into the FSWOL. Figure 2-1 shows an illustration of the PZR Safety Nozzle A indications. As shown in Figure 2-1, indications 1 and 1A are outside the ISI examination volume code coverage box but within the ABCD inspection box. Per Reference [8], disposition of indications 1 and 1A can be performed using the rules of ASME B&PV Code Section XI, IWB 3514 [2] using the full thickness of the nozzle and the overlay. Table 2-1 shows that indications 1 and 1A of PZR Safety Nozzle A meet the acceptance standard of IWB-3514. The evaluation in Table 2-1 evaluates the indications as found. Section 5.0 shows disposition of PZR Safety Nozzle A indications 1 and 1A in accordance with acceptance rules of ASME B&PV Code Section XI, IWB-3640 [2]. The results of the flaw evaluations in Section 5.0 provide flaw growth due fatigue. Flaw evaluation of the final flaw size is performed using the limit load analysis method of Appendix C of ASME B&PV Code Section XI [2].

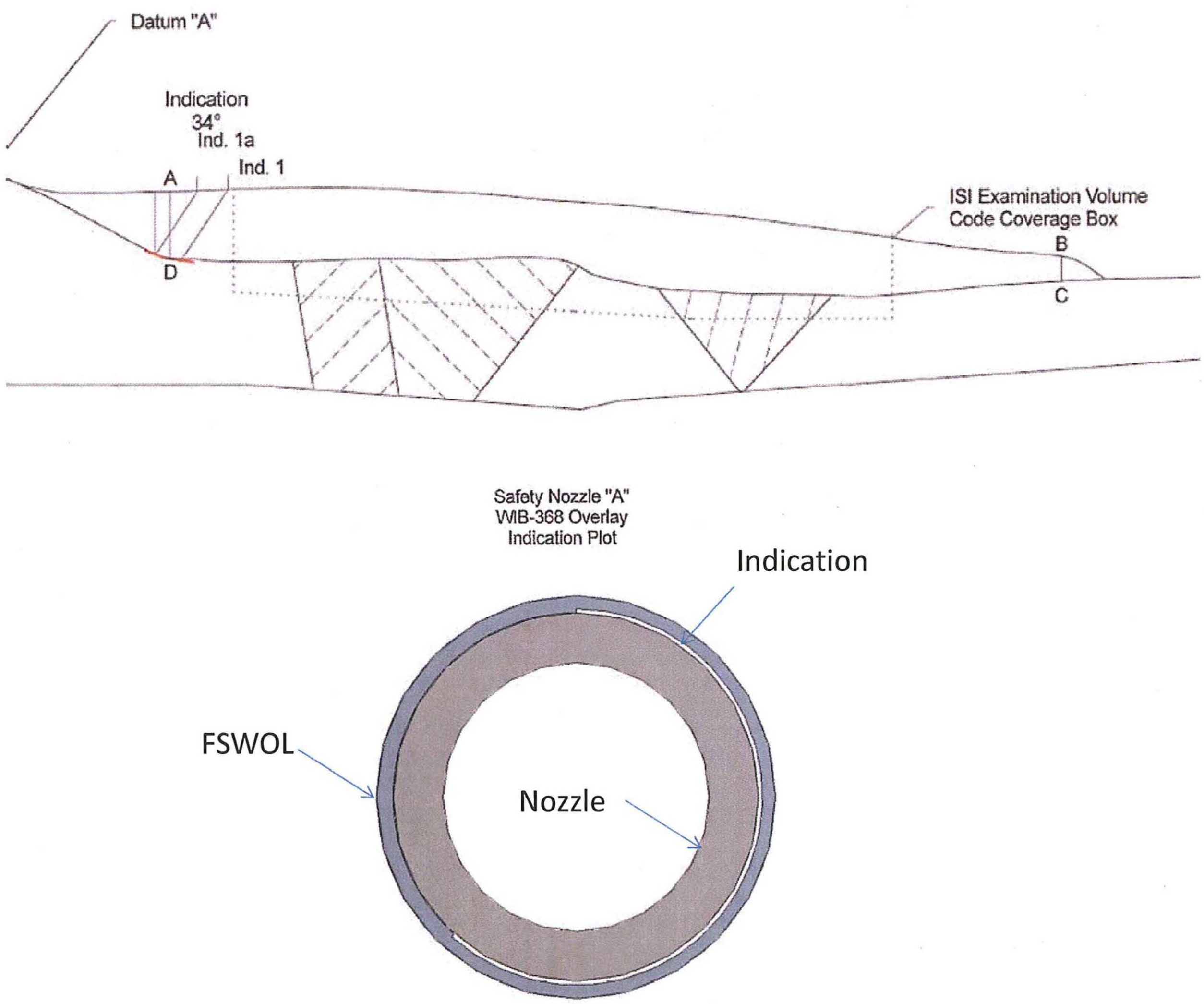

Figure 2-1: Illustration of Planar Projection of PZR Safety Nozzle A Indications.

Table 2-1: PZR Safety Nozzle A – IWB 3514 Acceptance Examination

Nozzle	Indication	Flaw Size 2a (in)	Half Flaw Size a (in)	Flaw Length l (in)	Thickness t (in)	Flaw Depth S (in)	Actual a/l	Actual a/t	Y =(S/t)/(a/t) = S/a Y	Y =min(Y,1)	0.4d	Check Proximity S > 0.4d			a/l- 0.00	a/l+ 0.05	Interp for a/l	Allowed a/t	Pass / Fail
Safety A	1	**0.08**	0.04	**16.3**	**1.61**	**0.6**	0.0025	**2.48%**	15	1	0.016	Y	t-	1	8.5	8.6	8.50	8.2%	Pass
	Circ												t+	2	8	8.2	8.01		

Nozzle	Indication	Flaw Size 2a (in)	Half Flaw Size a (in)	Flaw Length l (in)	Thickness t (in)	Flaw Depth S (in)	Actual a/l	Actual a/t	Y =(S/t)/(a/t) = S/a Y	Y =min(Y,1)	0.4d	Check Proximity S > 0.4d			a/l- 0.05	a/l+ 0.1	Interp for a/l	Allowed a/t	Pass / Fail
Safety A	1	**0.08**	0.04	**0.4**	**1.61**	**0.6**	0.1000	**2.48%**	15	1	0.016	Y	t-	1	8.6	8.8	8.80	8.5%	Pass
	Axial												t+	2	8.2	8.3	8.30		

Nozzle	Indication	Flaw Size 2a (in)	Half Flaw Size a (in)	Flaw Length l (in)	Thickness t (in)	Flaw Depth S (in)	Actual a/l	Actual a/t	Y =(S/t)/(a/t) = S/a Y	Y =min(Y,1)	0.4d	Check Proximity S > 0.4d			a/l- 0.00	a/l+ 0.05	Interp for a/l	Allowed a/t	Pass / Fail
Safety A	1A	**0.08**	0.04	**16.3**	**1.61**	**0.52**	0.0025	**2.48%**	13	1	0.016	Y	t-	1	8.5	8.6	8.50	8.2%	Pass
	Circ												t+	2	8	8.2	8.01		

Nozzle	Indication	Flaw Size 2a (in)	Half Flaw Size a (in)	Flaw Length l (in)	Thickness t (in)	Flaw Depth S (in)	Actual a/l	Actual a/t	Y =(S/t)/(a/t) = S/a Y	Y =min(Y,1)	0.4d	Check Proximity S > 0.4d			a/l- 0.05	a/l+ 0.10	Interp for a/l	Allowed a/t	Pass / Fail
Safety A	1A	**0.08**	0.04	**0.4**	**1.61**	**0.52**	0.1000	**2.48%**	13	1	0.016	Y	t-	1	8.6	8.8	8.80	8.5%	Pass
	Axial												t+	2	8.2	8.3	8.30		

In Table 2-1 the first column identifies the inspected nozzle and the second column identifies the label of the detected rejectable indication. The notations in Table 2-1 are described as the following: *2a* is the measured flaw size and *a* is half the flaw size, *l* is the measured flaw length, *t* is overlaid nozzle thickness used for evaluation (FSWOL + underlying original material thicknesses), *S* is the distance of subsurface flaw measured from the OD of the FSWOL, *a/l* is the calculated flaw aspect ratio, *a/t* is the actual flaw size to thickness ratio in percentage (%).

The overlaid nozzle thickness and flaw dimensions are used to look up the allowable flaw depth to thickness ratio from ASME B&PV Code Section XI, Table IWB 3514-2 [2]. In order to use ASME B&PV Code Section XI, Table IWB 3514-2, *Y* is calculated in accordance with ASME B&PV Code Section XI, Table IWB 3514-2, which is given by $Y=(S/t)/(a/t)=S/a$. From the foot notes of ASME B&PV Code Section XI, Table IWB 3514-2 if $Y > 1$ then $Y = 1$. It is necessary to examine the proximity rule to determine if the flaw can be treated as subsurface or surface flaw. Table 2-1 shows the proximity rule examination. To check the proximity rule, the quantity $0.4d$ is calculated, where *d* is the half flaw depth of subsurface flaw as shown in ASME B&PV Code Section XI, Figure IWA-3310-1. If *S* is greater than $0.4d$ then the flaw is treated as a subsurface flaw, else the flaw will be treated as surface flaw with depth $2d+S$.

Once the flaw is characterized as either subsurface or surface flaw, the overlaid nozzle thickness and flaw dimensions are used to look up the allowable flaw depth to thickness ratio from ASME B&PV Code Section XI, Table IWB 3514-2 [2]. To get the proper allowable flaw depth to thickness ratio, interpolation is necessary. For the thickness of interest, the thickness values that are just below and just above the thickness of interest are identified in ASME B&PV Code Section XI, Table IWB 3514-2. These thicknesses are labeled as t^- and t^+ in Table 2-1. t^- is the thickness column in ASME B&PV Code Section XI, Table IWB 3514-2 for the thickness just below the thickness of interest and t^+ is the thickness column in ASME B&PV Code Section XI, Table IWB 3514-2 for the thickness just above the thickness of interest. For the flaw aspect ratio (*a/l*) of interest, the flaw aspect ratio just above and just below the aspect ratio of interest are identified in ASME B&PV Code Section XI, Table IWB 3514-2. These aspect ratios are designated as al^- and al^+. a/l^- is the ASME B&PV Code Section XI, Table IWB 3514-2 flaw aspect ratio just below the flaw aspect ratio (*a/l*) of interest and a/l^+ is the ASME B&PV Code Section XI, Table IWB 3514-2 flaw aspect ratio just above the flaw aspect ratio (*a/l*) of interest. Therefore, for each pair of thickness and *a/l*, four pairs of allowable *a/t* ratios are looked up from ASME B&PV Code Section XI, Table IWB 3514-2 [an allowable *a/t* for each of (t^-, a/l^-), (t^+, a/l^-), (t^-, a/l^+), (t^+, a/l^+)].

The first interpolations is done on *a/l* which results in two interpolated values of allowable *a/t*. The second interpolation is performed on *t* which results in the desired allowable *a/t*.

2.1.2 PZR Safety Nozzle B Inspection

PZR Safety Nozzle B inspection revealed three laminar flaws. The disposition of PZR Safety Nozzle B laminar flaws in accordance with the rules of ASME B&PV Code Section XI, IWA-3360 and IWB-3514 is performed in Reference [3]. PZR Safety Nozzle B inspection also shows an NDE occlusion zone where lack of NDE coverage exists. The occlusion area was characterized by the sketch shown in Figure 2-2. As seen in Figure 2-2, the PZR Safety Nozzle B NDE occlusion area is located near the left edge of the ISI examination volume code coverage box. However, the PZR Safety Nozzle B NDE occlusion zone is located entirely in the low alloy steel nozzle. The planar dimensions of the bounding box of the occlusion area are 0.26 inch in the radial direction and 0.20 inch in the axial direction. Per Reference [8], disposition of postulated axial and circumferential flaws in PZR Safety Nozzle B NDE occlusion zone can be performed in accordance with the rules of ASME B&PV Code Section XI, IWB 3514 [2] using the full thickness of the nozzle and overlay. Table 2-2 shows that both axial and circumferential postulated flaws in PZR Safety Nozzle B NDE occlusion zone meet the acceptance standard of IWB-3514. Table 2-2 evaluates the as found indications. Section 5.0 shows disposition of PZR Safety Nozzle B NDE occlusion zone indications postulated flaws in accordance with the ASME B&PV Code Section XI, IWB-3640 [2] acceptance rules. The results of the flaw evaluations in Section 5.0 provide flaw growth due to fatigue. Flaw evaluation of the final flaw size is performed using the limit load analysis method of Appendix C of the ASME B&PV Code Section XI [2].

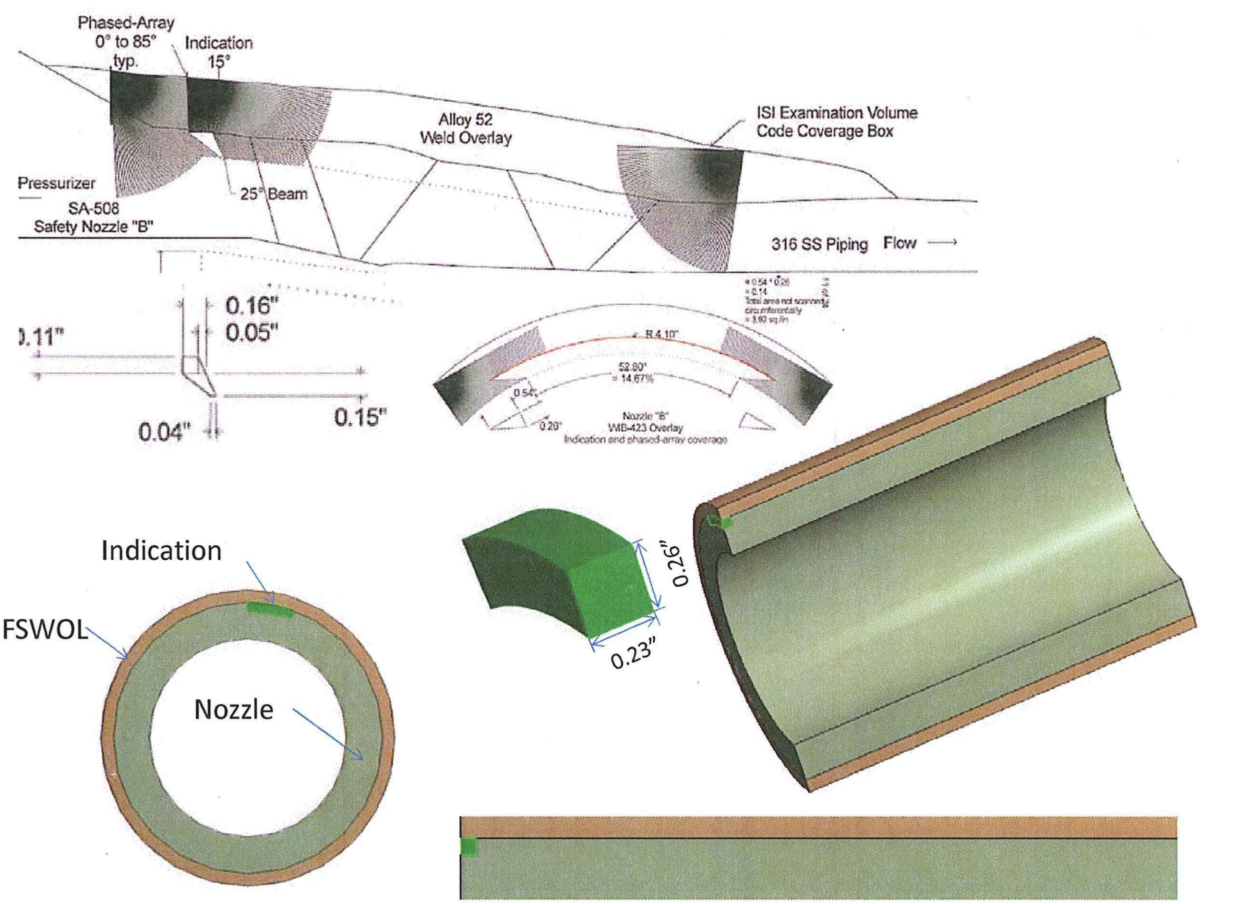

Figure 2-2: Illustration of Planar Projection of PZR Safety Nozzle B NDE Occlusion Zone

Table 2-2: PZR Safety Nozzle B – IWB 3514 Acceptance Examination

Nozzle	Indication	Flaw Size 2a (in)	Half Flaw Size a (in)	Flaw Length l (in)	Thickness t (in)	Flaw Depth S (in)	Actual a/l	Actual a/t	Y =(S/t)/(a/t) = S/a Y	Y =min(Y,1)	0.4d	Check Proximity S > 0.4d			a/l-	a/l+	Interp for a/l	Allowed a/t	Pass / Fail
															0.00	0.05			
Safety B	Circ	**0.26**	0.13	**5.5**	**1.61**	**0.58**	0.0236	**8.07%**	4.461538	1	0.052	Y	t-	1	8.5	8.6	8.55	8.3%	Pass
													t+	2	8	8.2	8.09		

Nozzle	Indication	Flaw Size 2a (in)	Half Flaw Size a (in)	Flaw Length l (in)	Thickness t (in)	Flaw Depth S (in)	Actual a/l	Actual a/t	Y =(S/t)/(a/t) = S/a Y	Y =min(Y,1)	0.4d	Check Proximity S > 0.4d			a/l-	a/l+	Interp for a/l	Allowed a/t	Pass / Fail
															0.50	0.50			
Safety B	Axial	**0.26**	0.13	**0.2**	**1.61**	**0.58**	0.6500	**8.07%**	4.461538	1	0.052	Y	t-	1	10	10	10.00	9.6%	Pass
													t+	2	9.4	9.4	9.40		

Note: for a/l > 0.5, a/l = 0.5 is used to lookup allowable a/t from ASME B&PV Code Section XI, Table IWB 3514-2.

2.1.3 PZR Safety Nozzle C Inspection

PZR Safety Nozzle C inspection revealed two small laminar indications (indications #3 and #4 per Reference [1]) that were found to be acceptable per the inspection report. PZR Safety Nozzle C inspection shows an NDE occlusion area, similar to that shown in Safety Nozzle B. The observed NDE occlusion zone shows lack of NDE coverage. The NDE occlusion zone of PZR Safety Nozzle C is characterized by the sketch shown in Figure 2-3. The Safety Nozzle C NDE occlusion area is located in the FSWOL near the safe end to stainless steel weld (SSW). The planar dimensions of the bounding box of the occlusion area are 0.21 inch in the radial direction and 0.25 inch in the axial direction. The occlusion zone length in the circumferential direction is 2.0 inch. Per Reference [8], disposition of postulated axial and circumferential flaws in PZR Safety Nozzle C NDE occlusion zone is to be performed in accordance with the rules of ASME B&PV Code Section XI, IWB 3514 [2] using the full thickness of the FSWOL and the underlying material. Table 2-3 shows that both axial and circumferential postulated flaws in PZR Safety Nozzle C NDE occlusion zone meet the acceptance standard of ASME B&PV Code Section XI, IWB-3514 [2]. The flaws postulated in PZR Safety Nozzle C NDE occlusion zone are also evaluated using the rules of ASME B&PV Code Section XI, IWB-3640 [2]. The results of the flaw evaluations in Section 5.0 provide flaw growth due to fatigue. Flaw evaluation of the final flaw size is performed using the limit load analysis method of Appendix C of the ASME B&PV Code Section XI.

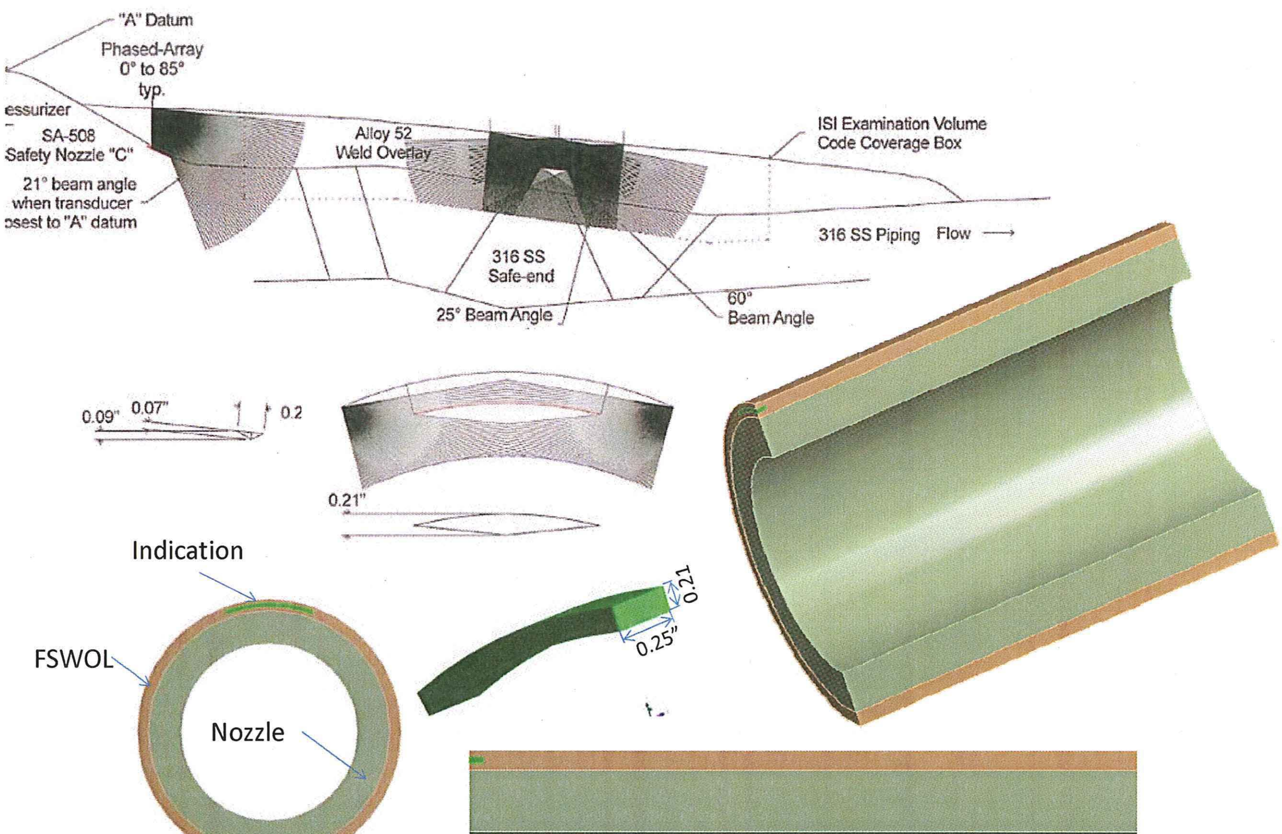

Figure 2-3: Illustration of Planar Projection of PZR Safety Nozzle C NDE Occlusion Zone

Table 2-3: PZR Safety Nozzle C – IWB 3514 Acceptance Examination

Nozzle	Indication	Flaw Size 2a (in)	Half Flaw Size a (in)	Flaw Length l (in)	Thickness t (in)	Flaw Depth S (in)	Actual a/l	Actual a/t	Y =(S/t)/(a/t) = S/a Y	Y =min(Y,1)	0.4d	Check Proximity S > 0.4d			a/l- 0.05	a/l+ 0.10	Interp for a/l	Allowed a/t	Pass / Fail
Safety C	Circ	**0.21**	0.105	**2**	**1.58**	**0.3**	0.0525	**6.65%**	2.857143	1	0.042	Y	t-	1	8.6	8.8	8.61	8.4%	Pass
													t+	2	8.2	8.3	8.21		

Nozzle	Indication	Flaw Size 2a (in)	Half Flaw Size a (in)	Flaw Length l (in)	Thickness t (in)	Flaw Depth S (in)	Actual a/l	Actual a/t	Y =(S/t)/(a/t) = S/a Y	Y =min(Y,1)	0.4d	Check Proximity S > 0.4d			a/l- 0.40	a/l+ 0.50	Interp for a/l	Allowed a/t	Pass / Fail
Safety C	Axial	**0.21**	0.105	**0.25**	**1.58**	**0.3**	0.4200	**6.65%**	2.857143	1	0.042	Y	t-	1	9.7	9.8	9.72	9.4%	Pass
													t+	2	9.1	9.3	9.14		

2.1.4 PZR Spray Nozzle Inspection

PZR Spray Nozzle inspection revealed one rejectable laminar indication. The disposition of PZR Spray Nozzle laminar flaws in accordance with the rules of ASME B&PV Code Section XI, IWA-3360 and IWB-3514 are performed in Reference [3]. PZR Spray Nozzle inspection revealed an NDE occlusion area, similar to that seen in Safety Nozzles B and C. The observed NDE occlusion zone shows lack of NDE coverage. The NDE occlusion zone of PZR Spray Nozzle is characterized by the sketch shown in Figure 2-4. The Spray Nozzle NDE occlusion area is located outside the FSWOL in the safe end to pipe weld (SSW). The planar dimensions of the bounding box of the Spray Nozzle occlusion area are 0.15 inch in the radial direction and 0.31 inch in the axial direction. The length of occlusion zone in the circumferential direction is 20.6 inch. As seen in Figure 2-4, the postulated flaws in the PZR Spray Nozzle occlusion zone are located in the ISI examination volume code coverage box but not within the volume of the FSWOL. Per Reference [8], disposition of postulated axial and circumferential flaws in PZR Spray Nozzle NDE occlusion zone is to be performed in accordance with the rules of ASME B&PV Code Section XI, IWB 3514 [2] using the thickness of the FSWOL and the underlying material. Table 2-4 shows that both axial and circumferential postulated flaws in PZR Spray Nozzle NDE occlusion zone meet the acceptance standard of ASME B&PV Code Section XI, IWB-3514 [2]. The flaws postulated in PZR Spray Nozzle NDE occlusion zone are also evaluated using the rules of ASME B&PV Code Section XI, IWB-3640 [2]. The results of the flaw evaluations in Section 5.0 provide flaw growth due to fatigue. Flaw evaluation of the final flaw size is performed using the limit load analysis method of Appendix C of the ASME B&PV Code Section XI.

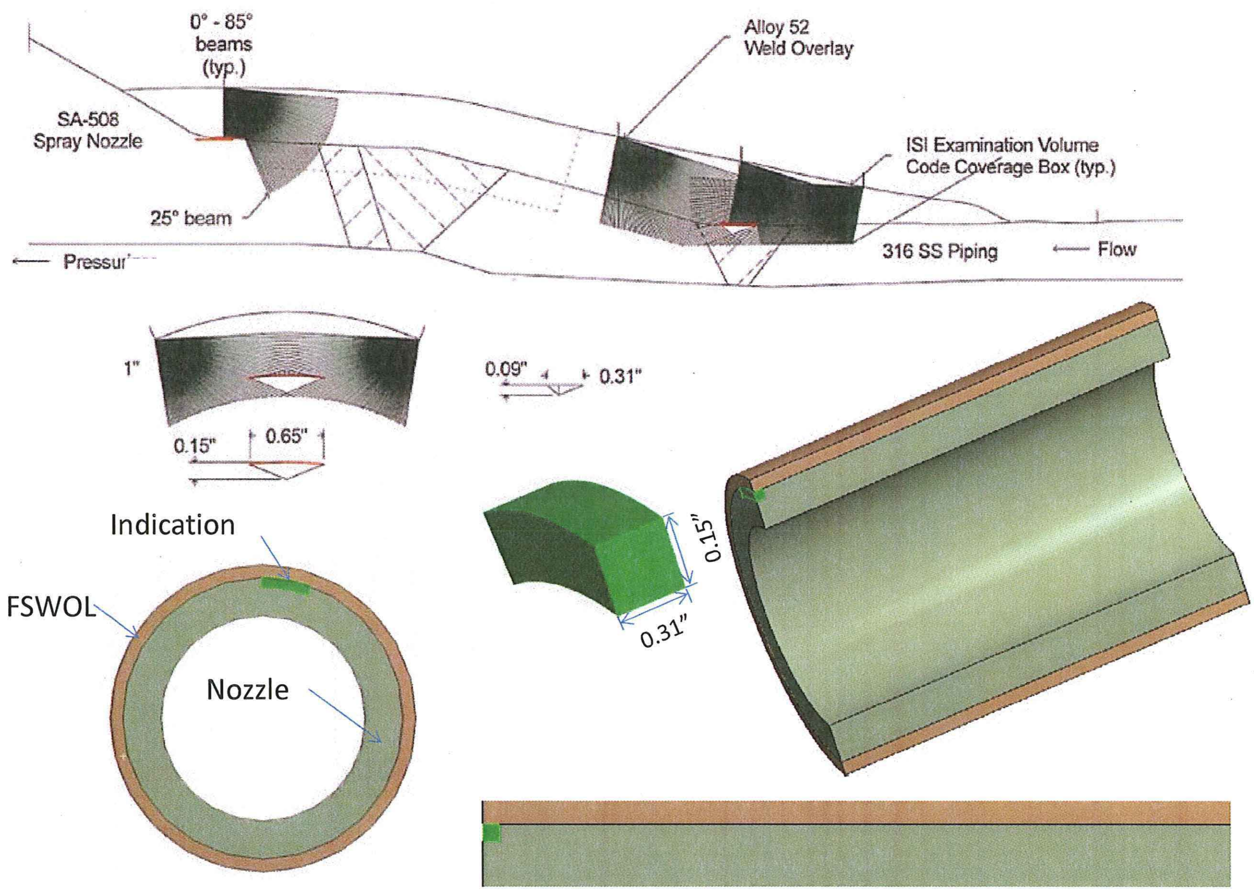

Figure 2-4: Illustration of Planar Projection of PZR Spray Nozzle NDE Occlusion Zone

Table 2-4: PZR Spray Nozzle – IWB 3514 Acceptance Examination

												Check					Interp for		
		Flaw Size	Half Flaw Size	Flaw Length	Thickness	Flaw Depth	Actual	Actual	Y =(S/t)/(a/t) = S/a			Proximity			a/l-	a/l+	a/l	Allowed	Pass / Fail
Nozzle	Indication	2a (in)	a (in)	l (in)	t (in)	S (in)	a/l	a/t	Y	Y =min(Y,1)	0.4d	S > 0.4d			0.00	0.05		a/t	
Spray	Circ	0.15	0.075	20.6	1.1	0.51	0.003641	6.82%	6.8	1	0.03	Y	t-	1	8.5	8.6	8.51	8.5%	Pass
													t+	2	8	8.2	8.01		

												Check					Interp for		
		Flaw Size	Half Flaw Size	Flaw Length	Thickness	Flaw Depth	Actual	Actual	Y =(S/t)/(a/t) = S/a			Proximity			a/l-	a/l+	a/l	Allowed	Pass / Fail
Nozzle	Indication	2a (in)	a (in)	l (in)	t (in)	S (in)	a/l	a/t	Y	Y =min(Y,1)	0.4d	S > 0.4d			0.20	0.25		a/t	
Spray	Axial	0.15	0.075	0.31	1.1	0.51	0.241935	6.82%	6.8	1	0.03	Y	t-	1	9.1	9.2	9.18	9.1%	Pass
													t+	2	8.6	8.7	8.68		

2.2 Summary of Indications

This section provides a summary of all indications with planar characteristic and postulated planar flaws in the NDE occlusion zones. Table 2-5 shows all indications and the results of the IWB-3514 evaluation. As seen in Table 2-5, all the postulated flaws in PZR Safety Nozzles and Spray Nozzle meet the acceptance standard of ASME B&PV Code Section XI, IWB 3514 [2].

Table 2-5: Summary of Indications

Nozzle	Indication	Flaw Direction	Flaw Size (in)	Flaw Length (in)	Thickness (in)	S	Meet IWB-3514
Safety A	1	Circ	0.08	16.3	1.61	0.60	Yes
Safety A	1	Axial	0.08	0.4	1.61	0.60	Yes
Safety A	1A	Circ	0.08	16.3	1.61	0.52	Yes
Safety A	1A	Axial	0.08	0.4	1.61	0.52	Yes
Safety B	Occlusion	Circ	0.26	5.50	1.61	0.58	Yes
Safety B	Zone	Axial	0.26	0.20	1.61	0.58	Yes
Safety C	Occlusion	Circ	0.21	2.00	1.58	0.3	Yes
Safety C	Zone	Axial	0.21	0.25	1.58	0.3	Yes
Spray	Occlusion	Circ	0.15	20.60	1.10	0.51	Yes
Spray	Zone	Axial	0.15	0.31	1.10	0.51	Yes

2.3 Postulated Flaw Shapes for Fracture Mechanics Evaluation

2.3.1 PZR Safety Nozzle A Indication

For PZR safety nozzle A indications, the idealized flaw shape for fracture mechanics evaluation is shown in Figure 2-5. The flaw is assumed as full 360° circumferential flaw that is embedded entirely in the FSWOL with one flaw tip located at the interface of the nozzle and the FSWOL and the other flaw tip extending 0.08 inch into the FSWOL.

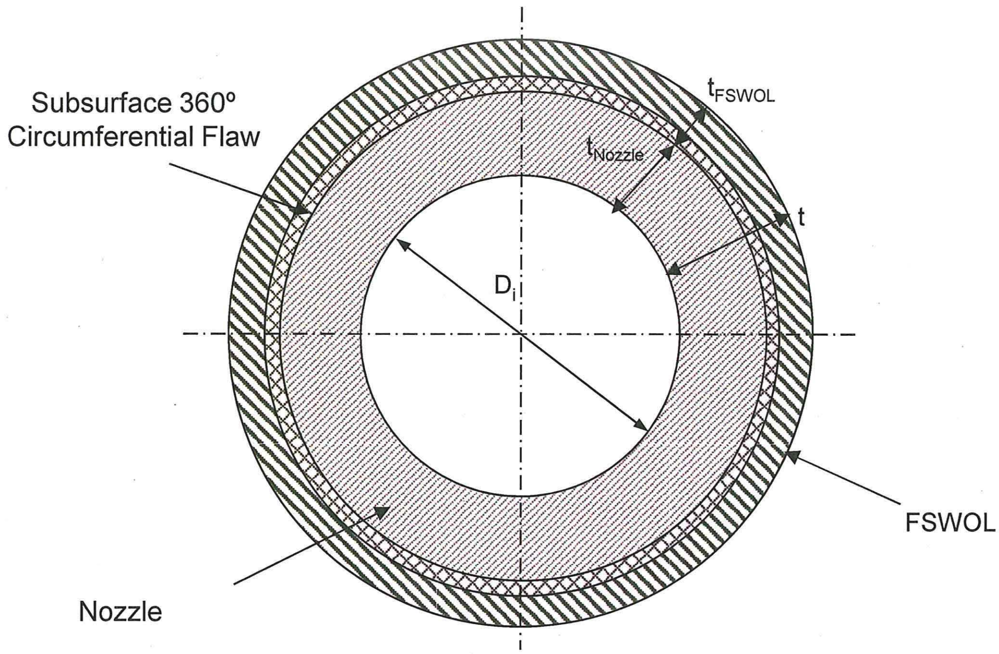

Figure 2-5: PZR Safety Nozzle A Idealized Indication

2.3.2 PZR Safety Nozzle B NDE Occlusion Area – Circumferential Flaw

For PZR safety nozzle B NDE occlusion area, the idealized circumferential flaw shape for fracture mechanics evaluation is shown in Figure 2-6. The flaw is assumed as full 360° circumferential flaw that is embedded entirely in the low alloy steel nozzle with one flaw tip located at the interface between the nozzle and the FSWOL and the other flaw tip extending 0.26 inch into low alloy steel nozzle.

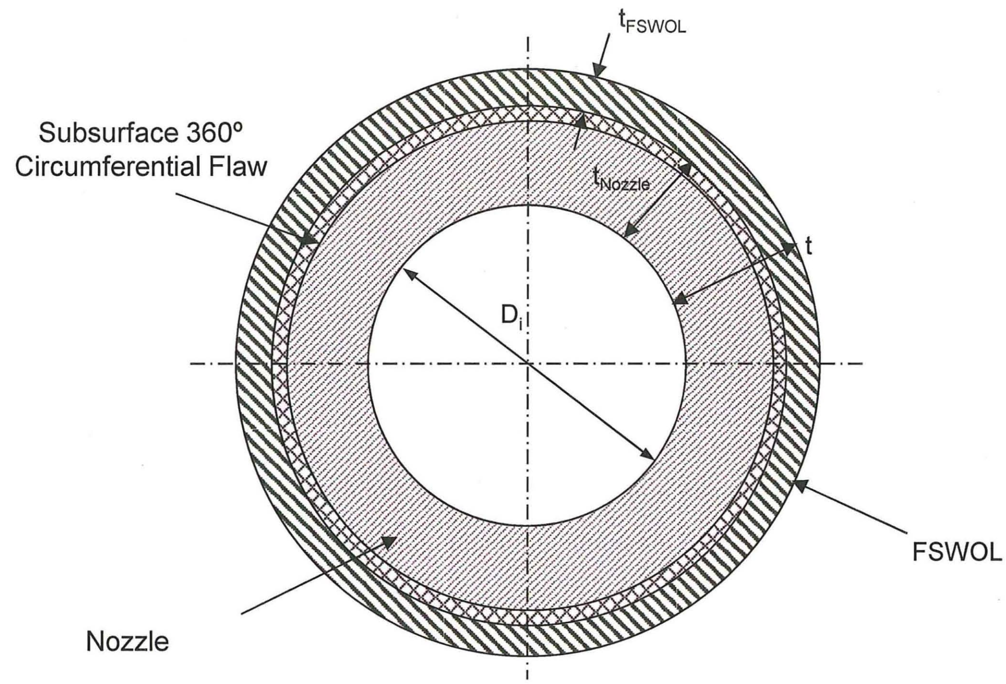

Figure 2-6: PZR Safety Nozzle B NDE Occlusion Area – Circumferential Direction

2.3.3 PZR Safety Nozzle B NDE Occlusion Area – Axial Flaw

For PZR safety nozzle B NDE occlusion area, the idealized axial flaw shape for fracture mechanics evaluation is shown in Figure 2-7. The flaw is assumed as an axial slit that extends through the full length of the nozzle. The axial flaw is embedded entirely in the low alloy steel nozzle with one flaw tip located at the interface between the nozzle and the FSWOL and the other flaw tip extending 0.26 inch into low alloy steel nozzle. It should be noted that the appropriate length for the postulated axial flaw is 0.23 inch. However, the fracture mechanics solution uses a length that extends through the full length of the nozzle, which is a conservative assumption.

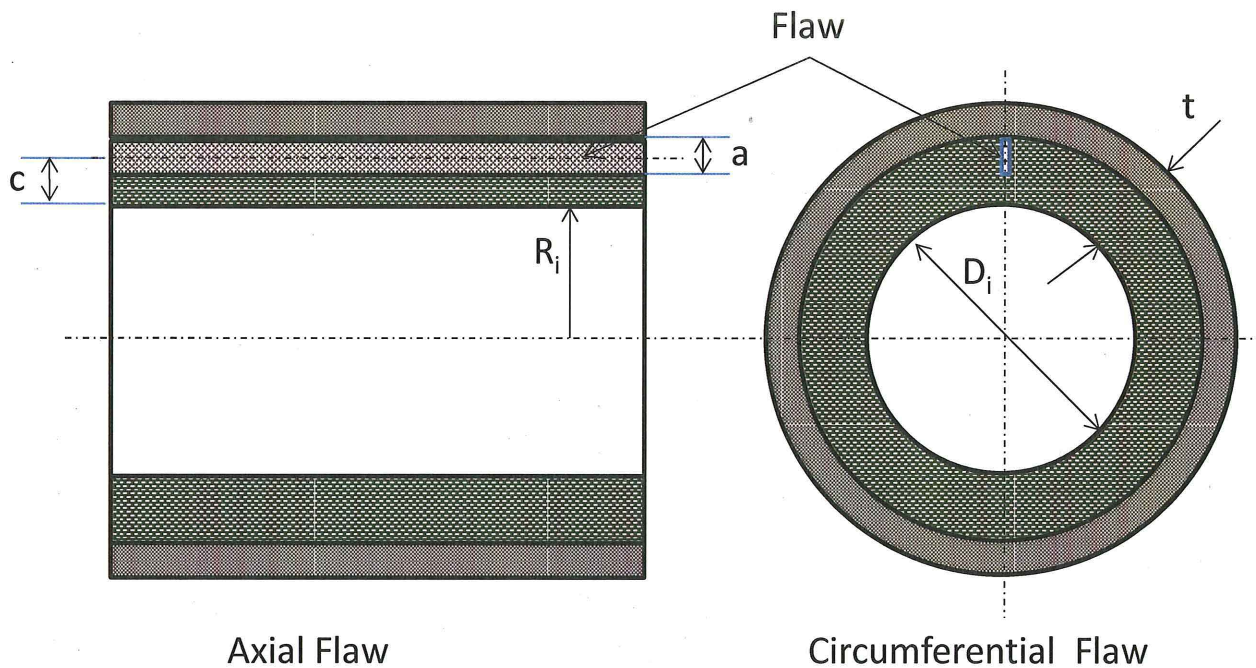

Figure 2-7: PZR Safety Nozzle B NDE Occlusion Area – Axial Direction

2.3.4 PZR Safety Nozzle C NDE Occlusion Area – Circumferential Flaw

For PZR safety nozzle C NDE occlusion area circumferential direction postulated indication, the idealized flaw shape for fracture mechanics evaluation is shown in Figure 2-8. The flaw is assumed as full 360° circumferential flaw that is embedded entirely in the FSWOL. The depth of the postulated flaw is 0.21 inch.

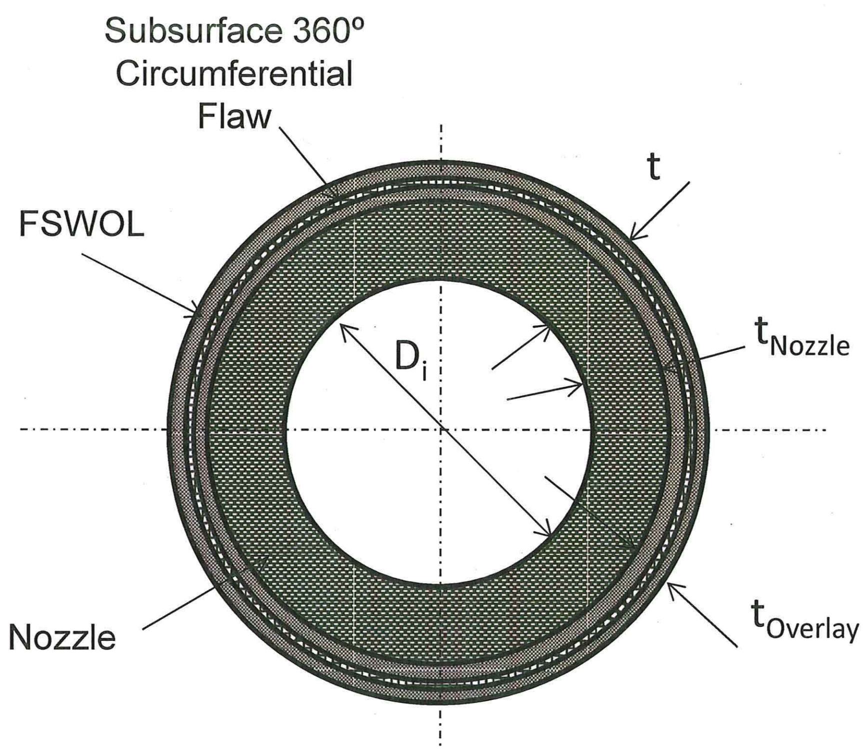

Figure 2-8: PZR Safety Nozzle C NDE Occlusion Area – Circumferential Direction

2.3.5 PZR Safety Nozzle C NDE Occlusion Area – Axial Flaw

For PZR safety nozzle C NDE occlusion area axial direction postulated indication, the idealized flaw shape for fracture mechanics evaluation is shown in Figure 2-9. The flaw is assumed as an axial slit that extends through the full length of the nozzle. The flaw is embedded entirely in the FSWOL. The flaw depth is 0.21 inch. It should be noted that the appropriate flaw length for the postulated flaw is 0.25 inch. However, the fracture mechanics solution uses a flaw length that extends through the full length of the nozzle, which is a conservative assumption.

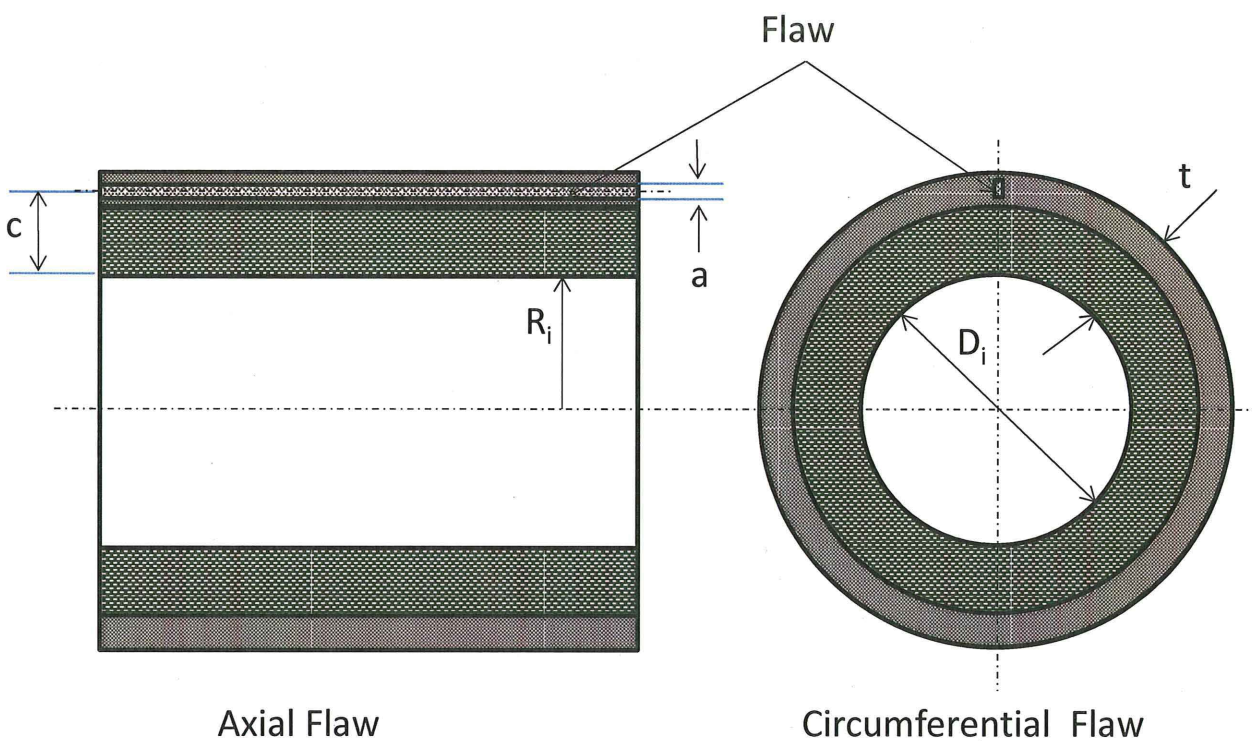

Figure 2-9: PZR Safety Nozzle C NDE Occlusion Area – Axial Direction

2.3.6 PZR Spray Nozzle Occlusion Area – Circumferential and Axial Flaws

For PZR Spray Nozzle, the NDE occlusion zone is inside the stainless steel weld (SSW) connecting the safe end to pipe spray line piping. The postulated flaws in the occlusion zone are in close proximity of the original FSWOL fracture mechanics qualification postulated flaws, which were assumed to be ID surface-connected flaws that extend through 75% of the SSW thickness. Therefore, the postulated flaws for the PZR Spray Nozzle occlusion zone are assumed to extend through the full thickness of the SSW. The postulated flaws are a full (360°) circumferential partial through-wall internal flaw in a cylinder as shown in Figure 2-10 and a semi-elliptical, inside surface connected axial flaw as shown in Figure 2-11. The axial flaw geometry is assumed to have 2:1 length to depth ratio. The postulated flaws will grow by fatigue in the FSWOL.

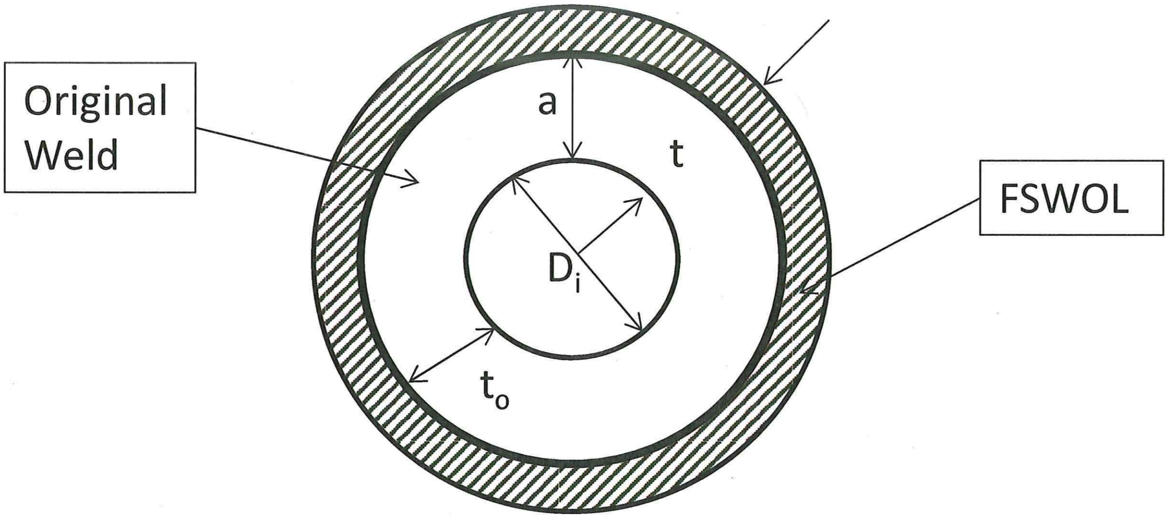

Figure 2-10: PZR Spray Nozzle Occlusion Zone – Circumferential Flaw

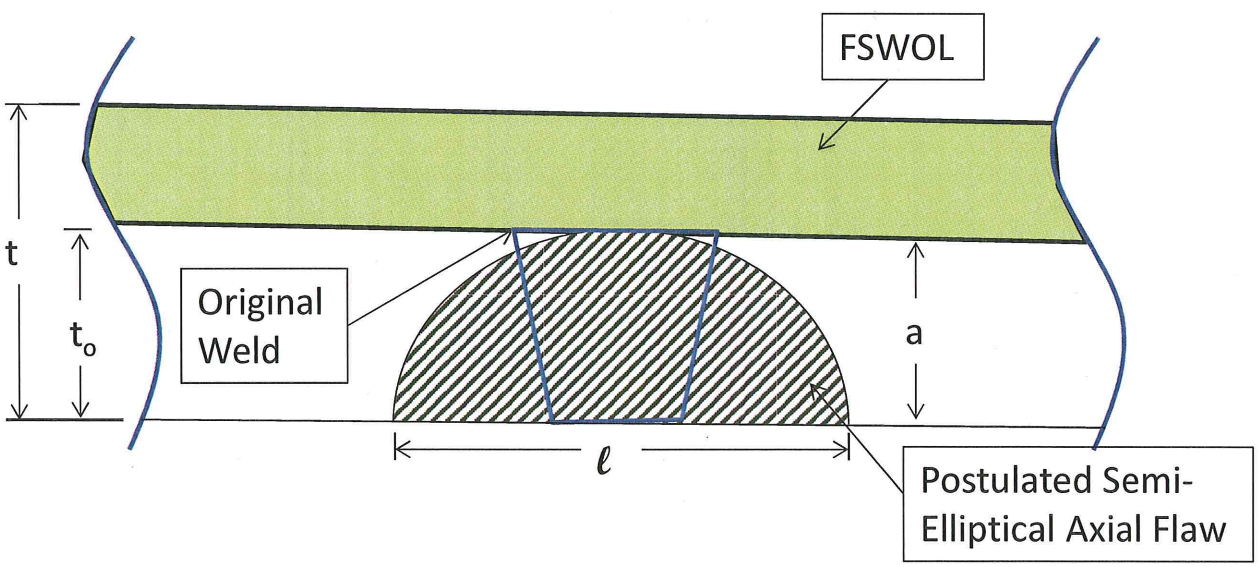

Figure 2-11: PZR Spray Nozzle Occlusion Zone – Axial Flaw

2.4 Geometry

The geometry parameters used in this document for the disposition of the observed indications are similar to the geometry parameters used in the original fracture mechanics qualification of the FSWOL designs described in Reference [9] for the PZR Safety Nozzle and in Reference [10] for the PZR Spray Nozzle. The original fracture mechanics qualifications for both of the PZR Safety and Spray Nozzles [9, 10] postulated both axial and circumferential inner surface-connected flaws along the four pathlines (FPath1, FPath2, FPath3, FPath4) shown in Figure 2-12 and Figure 2-13. Pertinent geometry parameters used in Reference [9] for analyzing the PZR Safety Nozzle, which were taken from References [11,12], are shown below in Table 2-6. The geometry parameters used in Reference [10] for analyzing the PZR Spray Nozzle, which were taken from References [13,14], are shown below in Table 2-7. For the current flaw dispositions, the PZR Safety and Spray Nozzles diameters and thickness are maintained as those used in References [9, 10]. It should be noted that the NDE inspection shows that the actual as-welded FSWOL thickness is greater than the minimum design FSWOL thickness used in References [9, 10]. Using the minimum design overlay thickness in the analysis of the flaw indications is conservative. The indications or NDE occlusion zone for PZR Safety Nozzles A and B are located close to FPath1 (Figure 2-12) while the NDE occlusion zone for PZR Safety Nozzle C is close to Fpath3 (Figure 2-12). The indications or NDE occlusion zone for PZR Spray Nozzle is located at FPath4 (Figure 2-13).

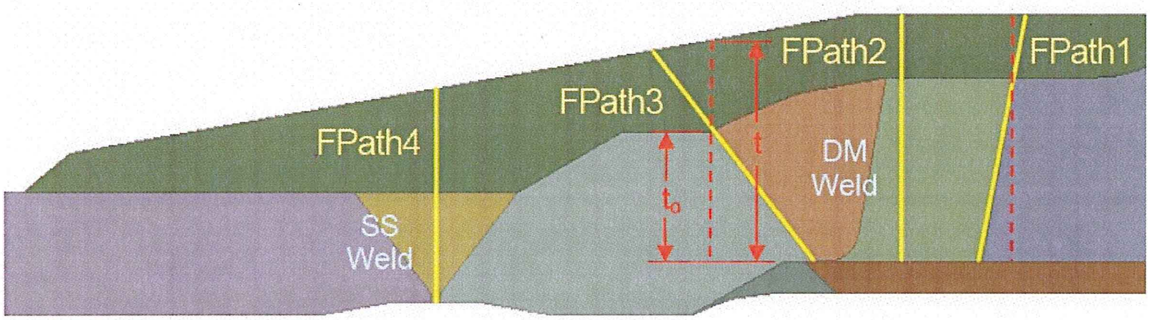

Figure 2-12: Safety Nozzle DM and SS Welds with Pathlines Superposed

Table 2-6: Safety Nozzle FSWOL Dimensions (Design)

[ ]

Note that the actual as welded FSWOL thickness is greater than the design thickness. The design thickness was conservatively used in crack growth analysis and evaluation of ASME B&PV Code, IWB-3640 acceptance rules.

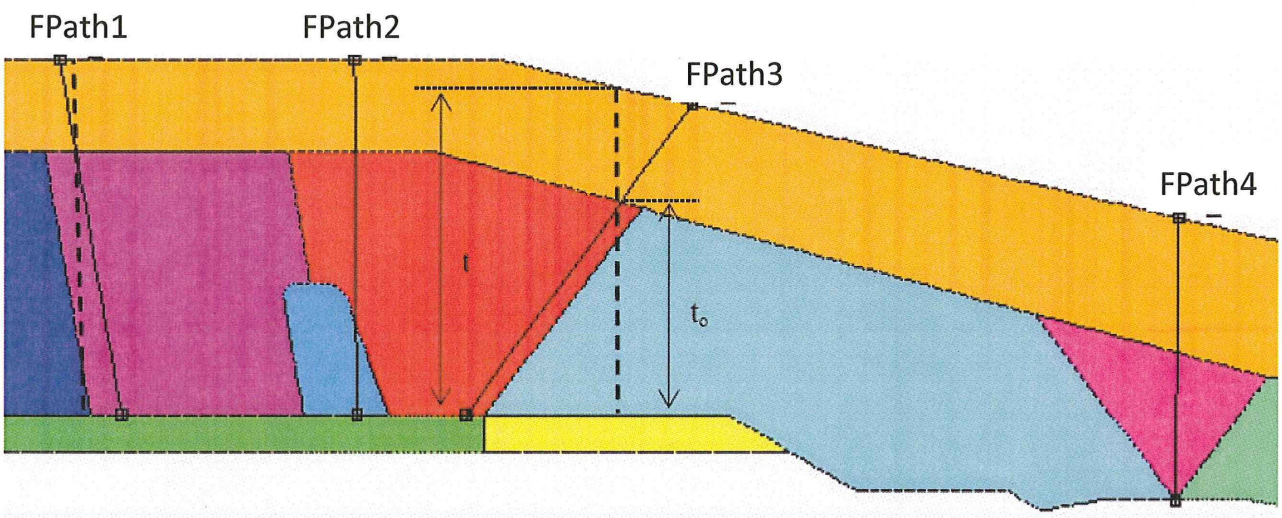

Figure 2-13: Spray Nozzle DM and SS Welds with Pathlines Superposed

Table 2-7: Spray Nozzle FSWOL Dimensions (Design)

[ ]

Note that the actual as welded FSWOL thickness is greater than the design thickness. The design thickness was conservatively used in crack growth analysis and evaluation of ASME B&PV Code, IWB-3640 acceptance rules.

2.5 Applied Stress Intensity Factor Calculation

This document used AREVACGC [15] to perform fatigue crack growth. AREVACGC [15] uses the weight function method for calculating the stress intensity factor (SIF). Calculating SIF using the weight function method is a well-established fracture mechanics methodology, which AREVA has incorporated into AREVACGC. The technical basis for this implementation is given in Reference [16]. AREVACGC computes the SIF internally and perform the fatigue crack growth to calculate the final flaw size at the end of the given service life. Necessary inputs to AREVACGC include nozzle geometry, flaw shape, size, orientation, applied stress, transient cycles, and temperature. The fatigue crack growth rates for the material of interest (low alloy steel nozzle and Alloy 52 FSWOL) are implemented in AREVACGC and can be activated by choosing appropriate input flags.

2.6 Applied Stresses

The categories of applied stresses that need to be considered are discussed in this section. As shown in Figure 2-12 and Figure 2-13, the pathlines chosen to sample the state of residual and operational stresses for the original fracture mechanics evaluations of the PZR Safety and Spray Nozzles FSWOL were selected in the welds and butter regions. FPath1 is the closest to the PZR Safety Nozzles A and B indications while FPath3 is the closest to the PZR Safety Nozzles C indications. FPath4 shown in Figure 2-13 is closest to the PZR Spray Nozzle indication.

2.6.1 Residual Stress in Welds

The residual stress profiles through the thickness of the DM weld, SS weld, and FSWOL are obtained from an analysis performed for the Diablo Canyon Unit 2 PZR Safety Nozzles [7] and PZR Spray Nozzle [17] . Stresses were obtained over multiple pathlines through the thickness of the DM weld, SS weld, and FSWOL. The pathlines over which these stresses are obtained are shown in Figure 2-12 for PZR Safety Nozzle and in Figure 2-13 for PZR Spray Nozzle. Axial and hoop residual stresses are obtained over these pathlines. The residual stresses at shutdown conditions are combined with the transient stress results to obtain the combined stresses over each pathline. These results are used to perform the fatigue crack growth calculation. For indications postulated in Safety Nozzle C, the residual stresses sampled along pathline FPath3 provide reasonable estimation of the residual stresses. For the indications postulated in Safety Nozzles A and B, the closest pathline for which residual stresses are extracted is pathline FPath1. However, upon reviewing the residual stress contour plots provided in Reference [7], it appears that the residual stresses in the region of interest is about 15-20 ksi higher than the residual stresses along pathline FPath1. To be conservative in estimating the appropriate residual stresses for the indications postulated in PZR Safety Nozzles A and B, a stress value of 25 ksi was added to the residual stresses reported along pathline FPath1. For the PZR Spray Nozzle indications, the residual stresses along pathline FPath4 from Reference [17] are used.

2.6.2 Sustained Stresses due to Piping Loads and System Pressure

2.6.2.1 PZR Safety Nozzle Piping Loads

The PZR Safety Nozzle Deadweight and Thermal loads applied at the safe end are obtained from the actual loads described in References [4,18]. They are given below:

Table 2-8: PZR Safety Nozzle Sustained Loads at the Safe End

[ ]

Note: The axial forces are aligned with the nozzle center line.

The loads applied at the safe end can be transferred conservatively to the cross section of interest along the nozzle. The region of interest for PZR Safety Nozzles A and B is approximately 4.09″ away from the safe end [11, 12]. The loads applied at the safe end can be transferred conservatively to the region of interest using a single moment arm of 4.09″. The transferred results are listed in Table 2-9. The transferred loads in Table 2-9 will be also used to analyze the indications in PZR Safety Nozzle C, which results in added conservatism.

Table 2-9: PZR Safety Nozzle Sustained Loads at the Nozzle

[ ]

Note: The axial forces are aligned with the nozzle center line.

Per Reference [18] the upset pressure is 2,600 psi and the normal operating pressure is 2250 psia. Crack face pressure is not added to the sustained loads of the Safety Nozzles indications since all indications are treated as subsurface flaws.

2.6.2.2 PZR Spray Nozzle Piping Loads

The PZR Spray Nozzle Deadweight and Thermal loads applied at the safe end are obtained from the actual loads described in References [5, 18]. They are given below:

Table 2-10: PZR Spray Nozzle Sustained Loads at the Safe End

[ ]

Note: The axial forces are aligned with the nozzle center line.

Per Reference [18] the upset pressure is 2,600 psi and the normal operating pressure is 2250 psia. The normal operating pressure is applied as a sustained crack face pressure for fatigue crack growth calculations. Also, since the PZR Spray Nozzle indications are near the SSW, the loads in Table 2-10 are used without transformation.

2.6.3 Transient Stresses

The cyclic operating stresses that are needed to calculate fatigue crack growth were obtained from a thermo elastic three-dimensional finite element analyses [6, 19]. These fatigue stresses were developed for each of the transients at a number of time points to capture the maximum and minimum stresses due to fluctuations in pressure and temperature. Per Reference [18], the number of RCS design transients is established for 60 years of design life. Using the design transient cycle counts results in a conservative number of remaining plant cycles relative to the actual cycles of each transient that the plant has experienced during the period of operation up to the installation of the weld overlays.

2.6.3.1 PZR Safety Nozzle Transient Stresses

Cyclic operating stresses for the PZR Safety Nozzles were generated in Reference [6] for the transients listed in Table 2-11. The PZR Safety Nozzles transient descriptions and cycle counts are given in Reference [6].

Table 2-11: Operating Transients for PZR Safety Nozzle

Designation	Transient Name	Design Cycles

Table 2-12: PZR Safety Nozzle Seismic (DE) loads at the Safe End

Table 2-13: PZR Safety Nozzle Seismic (DE) loads at the Nozzle

[ ]

2.6.3.2 PZR Spray Nozzle Transient Stresses

Cyclic operating stresses for the PZR Spray Nozzle were generated in Reference [19] for the transients listed in Table 2-14. The PZR Safety Nozzles transient descriptions and cycle counts are given in Reference [19].

Table 2-14: Operating Transients for PZR Spray Nozzle

Designation	Transient Name	Design Cycles

[ ]

Note (1): Leak Test is a substep of HU-LS.

Note (2): The heatup transient also includes [ ] spray actuations at a ΔT of [ ] °F arbitrarily and the Cooldown transient includes [ ] spray actuations at a ΔT of [ ] °F arbitrarily plus an additional [ ] spray actuation with a ΔT of -405°F after the pressurizer pressure is below [ ] psia. Therefore, the maximum number of cycles for heatup transients is conservatively set as the sum of the heatup transient ([ ]) plus the [ ] occurrences of heatup spray activations, which equals [ ] , and the maximum number of cycles for cooldown transients is conservatively set as the sum of the cooldown transient ([ ]) plus the [ ] occurrences of cooldown spray activations plus the [ ] additional occurrences of cooldown spray activations, which equals [ ] .

Note (3): An additional transient event due to seismic (DE) loads is also included for circumferential flaw analysis. The seismic stress conditions are taken to be the stresses of the transient condition with the highest Stress Intensity Factor of each path line plus / minus the stresses due to DE loads (Table 2-15)

Table 2-15: PZR Spray Nozzle Seismic (DE) loads at the Safe End

[ ]

2.7 Methodology for Flaw Growth Analyses

For the crack growth analyses, the applied stress intensity factor is driven by axial stress for the 360° circumferential flaw, and by hoop stress for the axial flaw. The relevant sources of stress for fatigue crack growth analyses are given below.

360° Circumferential Flaws	
Fatigue Crack Growth	Residual Axial Stress at Shutdown
	Axial Stress from Transients
	Sustained Stress due to Pipe Loads (Deadweight and Thermal)

Axial Flaws	
Fatigue Crack Growth	Residual Hoop Stress at Shutdown
	Hoop Stress from Transients

Flaw growth is calculated in one-year increments. As stated earlier a service life of 38 years is used in the current analysis. The highest metal temperature at the inside nozzle surface during a transient is used to determine the fatigue crack growth rate for each path line.

2.8 Fatigue Crack Growth (CG) Rates

2.8.1 Alloy 600 CG Rates in Air

Crack growth rates in air are used for subsurface flaws. Flaw growth due to cyclic loading is calculated using the fatigue crack growth model in Reference [20]. The crack growth rate (CGR) equation for Alloy 600 is given by

$$\left(\frac{da}{dN}\right)_{A600} = C_{A600} S_R (\Delta k)^n$$

where ΔK is the stress intensity factor range in terms of MPa√m and da/dN is the crack growth rate in the units of m/cycle. The other parameters are defined as

$$C_{A600} = 4.835x10^{-14} + 1.622x10^{-16}T - 1.490x10^{-18}T^2 + 4.355x10^{-21}T^3$$

$$S_R = (1 - 0.82R_{ratio})^{-2.2}$$

$$n = 4.1$$

$T =$ metal temperature in degrees Celcius

2.8.2 Alloy 600 CG Rates in PWR Environment

Crack growth rates in PWR environment are used for surface connected flaws. Flaw growth due to cyclic loading is calculated using the fatigue crack growth model in the NRC flaw evaluation guidelines for Alloy 600 in a PWR environment, References [21] and [22], which is based on work that was presented in Reference [20]. The crack growth rate equation for Alloy 600 is given by

$$\left(\frac{da}{dN}\right)_{A600} = CS_R S_{ENV} (\Delta K)^n$$

where ΔK is the stress intensity factor range in terms of MPa√m and da/dN is the crack growth rate in the units of m/cycle. The other parameters are defined as

$$C_{A600} = 4.835x10^{-14} + 1.622x10^{-16}T - 1.490x10^{-18}T^2 + 4.355x10^{-21}T^3$$

$$S_R = (1 - 0.82R_{ratio})^{-2.2}$$

$$S_{ENV} = 1 + A\left(CS_R \Delta K^n\right)^{m-1} T_R^{1-m}$$

$$A = 4.4X10^{-7}$$

$$n = 4.1$$

T = metal temperature in degrees Celcius

$$R_{ratio} = \frac{K_{min}}{K_{max}}$$

T_R = rise time in seconds, limited to a maximum of 5000 seconds Reference [20], or set to 30 seconds per reference [22]

2.8.3 Alloy 52 and 52M

In Reference [20], the available CGR data on Alloy 690 in air suggest that under similar loading conditions the CGR of Alloy 690 appears to be slightly higher than those of Alloy 600. However, the difference most likely is an artifact of a smaller database for Alloy 690. There are no data available for Alloy 52 and 52M in air. Before any data become available, a multiplier of 2 is applied for the crack growth rate of Alloy 52 and 52M upon those of Alloy 600.

$$\left(\frac{da}{dN}\right)_{A52/52M} = 2 \times \left(\frac{da}{dN}\right)_{A600}$$

2.9 Fatigue Crack Growth for Low-Alloy Steel Material

ASME B&PV Code Section XI provides fatigue crack growth for Low-Alloy Steel in air and primary water environments [2]. The formulation used for fatigue crack growth of low-Alloy steel material is provided in Article A-4000 of the Appendix A of Reference [2]. The fatigue crack growth rate da/dN of the material is characterized in terms of the range of applied stress intensity factor ΔK_I. The growth rate equation is

$$\frac{da}{dN} = C_0 (\Delta K_I)^n$$

where n is the slope of the log (da/dN) versus log(ΔK_I) and C_0 is a scaling constant depending on the environment and the R ratio.

Based on ASME B&PV Code Section XI , Article A-4300 [2], R =Kmin/Kmax.

For $0 \le R < 1$, $\Delta K_I = K_{max} - K_{min}$, and $S = 25.72 * (2.88 - R)^{-3.07}$.

For $-2 \le R < 0$, $\Delta K_I = K_{max}$, and $S = 1$.

For $R < -2$, $\Delta K_I = (1 - R)K_{max} / 3$, and $S = 1$.

The scaling constant C0 produces fatigue crack growth rates in units of in./cycle where ΔK_I is in units of $ksi\sqrt{in}$.

Reference fatigue crack growth behavior of material exposed to light-water reactor environments is given by the above rate equation with C_0 and n given by whichever of the following results in the higher fatigue crack growth rate da/dN: (1) the fatigue in air environment; (2) either of the following, as applicable.

First of all, determine the knee point of ΔK_I based on the R ratio (R =Kmin/Kmax if Kmin>0; R=0 if Kmin$\le$0).

$\Delta K_I^{knee} = 17.74 \quad (0 \le R \le 0.25)$,

$\Delta K_I^{knee} = 17.74[(3.75R + 0.06)/(26.9R - 5.725)]^{0.25} \quad (0.25 < R < 0.65)$,

and $\Delta K_I^{knee} = 12.04 \quad (0.65 \le R \le 1.0)$.

For low ΔK_I that $\Delta K_I \le \Delta K_I^{knee}$, $n = 5.95$ and $C_0 = 1.02 \times 10^{-12} S$, where S is given by

$$S = \begin{cases} 1.0 & (0 \le R \le 0.25) \\ 26.9R - 5.725 & (0.25 < R < 0.65) \\ 11.76 & (0.65 \le R < 1.0) \end{cases}.$$

For high ΔK_I that $\Delta K_I > \Delta K_I^{knee}$, $n = 1.95$ and $C_0 = 1.01 \times 10^{-7} S$, where S is given by

$$S = \begin{cases} 1.0 & (0 \le R \le 0.25) \\ 3.75R + 0.06 & (0.25 < R < 0.65). \\ 2.5 & (0.65 \le R < 1.0) \end{cases}$$

The above reference fatigue crack growth rate equations are intended for use when data from the actual product form are not available.

2.10 Methodology for Establishing Acceptance Flaw Sizes

First a flaw growth analysis is performed to establish the end-of-evaluation-period flaw depth a_f and flaw length l_f. Then the screening procedure in C-4000[2] is used to establish the failure mode and appropriate analysis methodology in determining the allowable flaw sizes. Per C-4000, flaws in austenitic weld metal or Ni-Cr-Fe weld metal should be evaluated using the austenitic piping flaw evaluation procedure given in C-5000[2] for non-flux welds and C-6000[2] for flux welds. The C-5000 procedure deals with ductile materials where the failure mode is that of plastic collapse at limit load while the C-6000 procedure addresses ductile materials which fracture by ductile flaw extension prior to reaching limit load.

The DM and SS welds in the Diablo Canyon Unit 2 PZR Safety and Spray Nozzles are considered to be flux welds and the FSWOL is considered to be a non-flux weld. Because all indications are located either in the FSWOL or at its boundary, both postulated circumferential and axial flaws, allowable flaw sizes are determined from respective tables in C- 5000[2].

Per Reference [18] the limiting load combinations for primary bending stress σ_b for the ASME B&PV Code Section XI Service Level conditions are as follows:

Service Level A (Normal) -	DW
Service Level B (Upset) -	DW + OBE
Service Level C (Emergency) -	No Transient or Load specified for this condition
Service Level D (Faulted) -	DW + DDE + HOSGRI (conservatively summed)

For the PZR Safety Nozzle, the loads applied at the safe end can be transferred to the nozzle by the moment arm of 4.09″ [11,12] and the results are listed in Table 2-16 and Table 2-17. For the PZR Spray Nozzle, the loads at the safe end are used. The PZR Spray Nozzle loads are listed in Table 2-18.

Table 2-16: PZR Safety Nozzle Loading Conditions for Primary Bending Stress, σ_b, at Safe End

[ ]

Note(1): The SRSS moment is defined as $\sqrt{M_y^2 + M_z^2}$

Table 2-17: PZR Safety Nozzle Loading Conditions for Primary Bending Stress, σ_b, at Nozzle

[ ]

Note(1): The SRSS moment is defined as $\sqrt{M_y^2 + M_z^2}$

Table 2-18: PZR Spray Nozzle Loading Conditions for Primary Bending Stress, σ_b, at Safe End

Note(1): The SRSS moment is defined as $\sqrt{M_y^2 + M_z^2}$

3.0 ASSUMPTIONS

This section discusses assumptions and modeling simplifications applicable to the present evaluation Diablo Canyon Unit 2 PZR Safety Nozzles indications.

3.1 Unverified Assumptions

There are no assumptions that must be verified before the present analysis can be used to support the disposition of the Diablo Canyon Unit 2 PZR Safety Nozzles indications.

3.2 Justified Assumptions

For the PZR Safety Nozzles A and B indications, the region of interest is located slightly away from the closest pathline (FPath1) stresses readily available [6]. Therefore a value of 25 ksi was added to both the axial and hoop components of the residual stresses along pathline FPath1. This is deemed to be a conservative estimation of the residual stresses in the region of interest for PZR Safety Nozzles A and B indications.

3.3 Modeling Simplification

For fatigue flaw growth analysis of circumferential indications, all circumferential indications are treated as full 360° indications. For fatigue flaw growth analysis of axial indications, all axial indications are treated as axial slits that extends through the full length of the evaluated nozzle. Theses simplifying assumption results in conservative SIF estimate for both circumferential and axial indications.

4.0 COMPUTER USAGE

4.1 Computer Software and Hardware

AREVACGC 5.0 was used in this document to compute fatigue crack growth. AREVACGC 5.0 installation was verified by running test cases 1 and 2 as documented below:

- Computer program tested: AREVACGC 5.0.
- Computer Hardware: Intel® Core® i7-2640M CPU @ 2.8 GHz Tag# 5VJV5S1
- Name of person running test: Samer Mahmoud
- Date of test: 2/27/2013.
- Results of the test: Both test cases produced were acceptable

4.2 Computer Files

Computer files of all analysis contained in this document are listed in Table 4-1. These files have been stored in COLDSTOR server within the directory [ ] ".

Table 4-1: Computer Files for Crack Growth Evaluation

[ ]

5.0 RESULTS OF INDICATIONS ANALYSES

5.1 PZR Safety Nozzle A Indications

5.1.1 PZR Safety Nozzle A Circumferential Flaw Growth Analysis

The calculated flaw growth for PZR Safety Nozzle A indications was negligible. Table 5-1 shows a summary of the predicted crack growth as calculated by AREVACGC. Table 5-2 shows the contribution of each analyzed transient to the calculated fatigue crack growth.

Table 5-1: PZR Safety Nozzle A Circumferential Flaw Growth - Summary

Initial Flaw Width (in) =	0.0800
Initial Flaw Center (in) =	1.1300
Final Flaw Width (in) =	0.0800
Final Flaw Center (in) =	1.1300
Growth towards Center (in) =	8.4073E-08
Growth away from Center (in) =	3.4210E-08
Total Amount of Fatigue Crack Growth (in) =	1.1828E-07

Table 5-2: PZR Safety Nozzle A Circumferential Flaw Growth – Detailed Analysis

Trans.	Growth (in)	Percent
	3.2891E-08	27.8071
	4.7577E-08	40.2230
	1.1017E-08	9.3138
	5.7562E-09	4.8665
	0.0000E+00	0.0000
	1.2378E-08	10.4645
	5.9569E-09	5.0361
	0.0000E+00	0.0000
	1.2960E-09	1.0956
	0.0000E+00	0.0000
	1.4116E-09	1.1934

5.1.2 PZR Safety Nozzle A Circumferential Final Flaw Size Evaluation

As seen in Section 5.1.1, flaw growth is negligible. Table 5-3 shows evaluation of the final flaw depth with flaw acceptance standard from Appendix C of the ASME B&PV Code Section XI [2]. It is seen from Table 5-3 that the final flaw size is much smaller than the allowable flaw size. Therefore, the indications found in PZR Safety Nozzle A are acceptable for the remainder of the plants service life.

Table 5-3: PZR Nozzle A Circumferential Final Flaw Size Evaluation

Allowable Flaw Depths	Normal	Upset	Faulted	Reference [2]
Service level maximum pressure, p, (psi)	[ ]	[ ]	[ ]	
Service level maximum temperature, T, (F)	[ ]	[ ]	[ ]	
Service level flow stress, $\sigma_f = (Sy+Su)/2$, (psi)	[ ]	[ ]	[ ]	
Total thickness, t , (inch)	[ ]	[ ]	[ ]	
Overlay outside diameter, D_o, (inch)	[ ]	[ ]	[ ]	
Sectional area, A, (inch^2)	[ ]	[ ]	[ ]	
Moment of inertia, I, (inch^4)	[ ]	[ ]	[ ]	
Section modulus, S (inch3)	[ ]	[ ]	[ ]	
Primary Bending Moment, $M_{b\ SRSS}$ (in-lbf)	[ ]	[ ]	[ ]	
Thermal Expansion Bending Moment, $M_{e\ SRSS}$ (in-lbf)	[ ]	[ ]	[ ]	
Safety factor, SFm,	2.7	2.4	1.3	C-2621
Safety factor, SFb,	2.3	2.0	1.4	C-2621
Calculated primary membrane stress, $\sigma_m = pD_o/4t$, (psi)	[ ]	[ ]	[ ]	C-2500
Calculated primary bending stress, σ_b = Moment SRSS/S , (psi)	[ ]	[ ]	[ ]	C-2500
Calculated secondary bending stress, σ_e = Moment SRSS/S, (psi)	[ ]	[ ]	[ ]	C-2500
Final Flaw Depth, a_f, (in)	0.080	0.080	0.080	
Final Flaw length, l_f, (in)	25.133	25.133	25.133	
Calculated final flaw depth to thickness ratio, a_f /t,	[ ]	[ ]	[ ]	
Stress ratio, $[\sigma_m + \sigma_b] / \sigma_f$	[ ]	[ ]	[ ]	C-5311
Ratio of flaw length to pipe circumference, $l_f / \pi D_o$,	[ ]	[ ]	[ ]	C-5311
Ratio of allowable flaw depth to thickness, a_{allow} / t,	0.750	0.750	0.748	Table C-5310-1,2,4
Allowable flaw depth, a_{allow} , (in)	1.095	1.095	1.092	

5.2 PZR Safety Nozzle B NDE Occlusion Zone

5.2.1 PZR Safety Nozzle B Circumferential Flaw Growth Analysis

The calculated flaw growth for the postulated circumferential flaw (representing NDE occlusion zone) in PZR Safety Nozzle B is found to be negligible. Table 5-4 shows a summary of the crack growth as calculated by AREVACGC. Table 5-5 shows the contribution of each analyzed transient to the calculated fatigue crack growth.

Table 5-4: PZR Safety Nozzle B Circumferential Flaw Growth - Summary

Initial Flaw Width (in) =	0.2700
Initial Flaw Center (in) =	0.9550
Final Flaw Width (in) =	0.2700
Final Flaw Center (in) =	0.9550
Growth towards Center (in) =	1.3506E-05
Growth away from Center (in) =	3.2844E-06
Total Amount of Fatigue Crack Growth (in) =	1.6791E-05

Table 5-5: PZR Safety Nozzle B Circumferential Flaw Growth – Detailed Analysis

Trans.	Growth (in)	Percent
	1.6383E-05	97.5725
	2.2487E-07	1.3392
	3.7190E-08	0.2215
	1.9604E-08	0.1168
	0.0000E+00	0.0000
	6.9646E-08	0.4148
	3.6598E-08	0.2180
	0.0000E+00	0.0000
	9.0028E-09	0.0536
	0.0000E+00	0.0000
	1.0685E-08	0.0636

5.2.2 PZR Safety Nozzle B Circumferential Final Flaw Size Evaluation

As seen in Section 5.2.1, the crack growth for postulated circumferential flaw is negligible. Table 5-6 shows evaluation of the final flaw depth with flaw acceptance standard from Appendix C of the ASME B&PV Code Section XI, [2]. It is seen from Table 5-6 that the final flaw size is much smaller than the allowable flaw size. Therefore, the indications found in PZR Safety Nozzle B are acceptable for the remainder of the plants service life.

Table 5-6: PZR Safety Nozzle B Circumferential Final Flaw Size Evaluation

Allowable Flaw Depths	Normal	Upset	Faulted	Reference [2]
Service level maximum pressure, p, (psi)	[ ]	[ ]	[ ]	
Service level maximum temperature, T, (F)	[ ]	[ ]	[ ]	
Service level flow stress, σ_f = (Sy+Su)/2, (psi)	[ ]	[ ]	[ ]	
Total thickness, t , (inch)	[ ]	[ ]	[ ]	
Overlay outside diameter, D_o, (inch)	[ ]	[ ]	[ ]	
Sectional area, A, (inch^2)	[ ]	[ ]	[ ]	
Moment of inertia, I, (inch^4)	[ ]	[ ]	[ ]	
Section modulus, S (inch3)	[ ]	[ ]	[ ]	
Primary Bending Moment, $M_{b\,SRSS}$ (in-lbf)	[ ]	[ ]	[ ]	
Thermal Expansion Bending Moment, $M_{e\,SRSS}$ (in-lbf)	[ ]	[ ]	[ ]	
Safety factor, SFm,	2.7	2.4	1.3	C-2621
Safety factor, SFb,	2.3	2.0	1.4	C-2621
Calculated primary membrane stress, σ_m = $pD_o/4t$, (psi)	[ ]	[ ]	[ ]	C-2500
Calculated primary bending stress, σ_b = Moment SRSS/S , (psi)	[ ]	[ ]	[ ]	C-2500
Calculated secondary bending stress, σ_e = Moment SRSS/S, (psi)	[ ]	[ ]	[ ]	C-2500
Final Flaw Depth, a_f , (in)	0.270	0.270	0.270	
Final Flaw length, l_f , (in)	25.133	25.133	25.133	
Calculated final flaw depth to thickness ratio, a_f /t,	[ ]	[ ]	[ ]	
Stress ratio, $[\sigma_m + \sigma_b] / \sigma_f$	[ ]	[ ]	[ ]	C-5311
Ratio of flaw length to pipe circumference, $l_f / \pi D_o$,	[ ]	[ ]	[ ]	C-5311
Ratio of allowable flaw depth to thickness, a_{allow} / t,	0.750	0.750	0.748	Table C-5310-1,2,4
Allowable flaw depth, a_{allow} , (in)	1.095	1.095	1.092	

5.2.3 PZR Safety Nozzle B Axial Flaw Growth Analysis

The calculated crack growth for postulated axial flaw (representing NDE occlusion region) in Safety Nozzle B is negligible. Table 5-7 shows a summary of the crack growth as calculated by AREVACGC. Table 5-8 shows the contribution of each analyzed transient to the calculated fatigue crack growth.

Table 5-7: PZR Safety Nozzle B Axial Flaw Growth - Summary

Initial Flaw Width (in) =	0.2700*
Initial Flaw Center (in) =	0.9550
Final Flaw Width (in) =	0.2700
Final Flaw Center (in) =	0.9550
Growth towards Center (in) =	1.1582E-05
Growth away from Center (in) =	5.2705E-06
Total Amount of Fatigue Crack Growth (in) =	1.6853E-05

**0.27 inch flaw size was used in the analysis. The actual flaw size is 0.26 inch. The analysis is conservative*

Table 5-8: PZR Safety Nozzle B Axial Flaw Growth – Detailed Analysis

Trans.	Growth (in)	Percent
	1.5544E-05	92.2361
	8.7848E-07	5.2128
	4.3991E-08	0.2610
	4.1646E-08	0.2471
	0.0000E+00	0.0000
	1.9026E-07	1.1289
	1.3341E-07	0.7916
	0.0000E+00	0.0000
	2.0629E-08	0.1224
	0.0000E+00	0.0000

5.2.4 PZR Safety Nozzle B Axial Final Flaw Size Evaluation

As seen in Section 5.2.3, there is virtually no flaw growth for the postulated axial flaw. Table 5-9 shows evaluation of the final flaw size with the flaw acceptance standard of Appendix C of the ASME B&PV Code Section XI. It is seen from Table 5-9 that the final flaw size is much smaller than the allowable flaw size. Therefore, the indications found in PZR Safety Nozzle B are acceptable for the remainder of the plants service life.

Table 5-9: PZR Safety Nozzle B Axial Final Flaw Size Evaluation

Allowable Flaw Depths	Normal	Upset	Faulted	Reference [2]
Service level maximum pressure, p, (psi)	[ ]	[ ]	[ ]	
Service level maximum temperature, T, (F)	[ ]	[ ]	[ ]	
Service level flow stress, $\sigma_f = (Sy+Su)/2$, (psi)	[ ]	[ ]	[ ]	
Total thickness, t , (inch)	[ ]	[ ]	[ ]	
Overlay outside diameter, Do, (inch)	[ ]	[ ]	[ ]	
Inside diameter, Di, (inch)	[ ]	[ ]	[ ]	
Mean pipe radius, Rm (inch)	[ ]	[ ]	[ ]	
Final Flaw Depth, a_f , (in)	0.270*	0.270*	0.270*	
Final flaw length, l_f (inch)	0.23	0.23	0.23	
Nondimensional flaw length, $l_f / (R_m t)^{0.5}$	[ ]	[ ]	[ ]	C-5410
Pipe hoop stress, $\sigma_h = pR_m/t$, (psi)	[ ]	[ ]	[ ]	C-5410
Stress ratio, σ_h / σ_f	[ ]	[ ]	[ ]	C-5410
Allowable flaw depth to thickness ratio, a_{allow}/t,	0.75	0.75	0.75	Table 5410-1
Final flaw depth to thickness ratio, a_f / t,	0.1849	0.1849	0.1849	

**0.27 inch flaw size was used in the analysis. The actual flaw size is 0.26 inch. The analysis is conservative*

5.3 PZR Safety Nozzle C NDE Occlusion Zone

5.3.1 PZR Safety Nozzle C Circumferential Flaw Growth Analysis

The calculated flaw growth for PZR Safety Nozzle C indications was negligible. Table 5-10 shows a summary of the crack growth as calculated by AREVACGC. Table 5-11 shows the contribution of each analyzed transient to the calculated fatigue crack growth.

Table 5-10: PZR Safety Nozzle C Circumferential Flaw Growth - Summary

Initial Flaw Width (in) =	0.2100
Initial Flaw Center (in) =	1.0310
Final Flaw Width (in) =	0.2113
Final Flaw Center (in) =	1.0305
Growth towards Center (in) =	1.1674E-03
Growth away from Center (in) =	1.2112E-04
Total Amount of Fatigue Crack Growth (in) =	1.2886E-03

Table 5-11: PZR Safety Nozzle C Circumferential Flaw Growth – Detailed Analysis

Trans.	Growth (in)	Percent
	1.2878E-03	99.9419
	4.5521E-07	0.0353
	6.9296E-08	0.0054
	4.2220E-08	0.0033
	0.0000E+00	0.0000
	8.7996E-08	0.0068
	6.6894E-08	0.0052
	0.0000E+00	0.0000
	1.4047E-08	0.0011
	0.0000E+00	0.0000
	1.2970E-08	0.0010

5.3.2 PZR Safety Nozzle C Circumferential Final Flaw Size Evaluation

As seen in Section 5.3.1, there is virtually no flaw growth. Table 5-12 shows evaluation of the final flaw size with the flaw acceptance standard of Appendix C of the ASME B&PV Code Section XI [2]. It is seen from Table 5-12 that the final flaw size is much smaller than the allowable flaw size. Therefore, the indications found in PZR Safety Nozzle C are acceptable for the remainder of the plants service life.

Table 5-12: PZR Safety Nozzle C Circumferential Final Flaw Size Evaluation

Allowable Flaw Depths	Normal	Upset	Faulted	Reference [2]
Service level maximum pressure, p, (psi)	[ ]	[ ]	[ ]	
Service level maximum temperature, T, (F)	[ ]	[ ]	[ ]	
Service level flow stress, $\sigma_f = (Sy+Su)/2$, (psi)	[ ]	[ ]	[ ]	
Total thickness, t , (inch)	[ ]	[ ]	[ ]	
Overlay outside diameter, D_o, (inch)	[ ]	[ ]	[ ]	
Sectional area, A, (inch^2)	[ ]	[ ]	[ ]	
Moment of inertia, I, (inch^4)	[ ]	[ ]	[ ]	
Section modulus, S (inch3)	[ ]	[ ]	[ ]	
Primary Bending Moment, $M_{b\,SRSS}$ (in-lbf)	[ ]	[ ]	[ ]	
Thermal Expansion Bending Moment, $M_{e\,SRSS}$ (in-lbf)	[ ]	[ ]	[ ]	
Safety factor, SFm,	2.7	2.4	1.3	C-2621
Safety factor, SFb,	2.3	2.0	1.4	C-2621
Calculated primary membrane stress, $\sigma_m = pD_o/4t$, (psi)	[ ]	[ ]	[ ]	C-2500
Calculated primary bending stress, σ_b = Moment SRSS/S , (psi)	[ ]	[ ]	[ ]	C-2500
Calculated secondary bending stress, σ_e = Moment SRSS/S, (psi)	[ ]	[ ]	[ ]	C-2500
Final Flaw Depth, a_f , (in)	0.211	0.211	0.211	
Final Flaw length, l_f , (in)	25.133	25.133	25.133	
Calculated final flaw depth to thickness ratio, a_f /t,	[ ]	[ ]	[ ]	
Stress ratio, $[\sigma_m + \sigma_b] / \sigma_f$	[ ]	[ ]	[ ]	C-5311
Ratio of flaw length to pipe circumference, $l_f / \pi D_o$,	[ ]	[ ]	[ ]	C-5311
Ratio of allowable flaw depth to thickness, a_{allow} / t,	0.750	0.750	0.748	Table C-5310-1,2,4
Allowable flaw depth, a_{allow} , (in)	1.095	1.095	1.092	

5.3.3 PZR Safety Nozzle C Axial Flaw Growth Analysis

The calculated flaw growth for postulated axial flaw representing NDE occlusion zone in PZR Safety Nozzle C was small. Table 5-13 shows a summary of the crack growth as calculated by AREVACGC. Table 5-14 shows the contribution of each analyzed transient to the calculated fatigue crack growth.

Table 5-13: PZR Safety Nozzle C Axial Flaw Growth - Summary

Initial Flaw Width (in) =	0.2100
Initial Flaw Center (in) =	1.0310
Final Flaw Width (in) =	0.2102
Final Flaw Center (in) =	1.0310
Growth towards Center (in) =	9.9282E-05
Growth away from Center (in) =	1.1137E-04
Total Amount of Fatigue Crack Growth (in) =	2.1065E-04

Table 5-14: PZR Safety Nozzle C Axial Flaw Growth – Detailed Analysis

Trans.	Growth (in)	Percent
	2.0852E-04	98.9878
	1.5578E-06	0.7395
	7.5528E-08	0.0359
	8.2739E-08	0.0393
	0.0000E+00	0.0000
	1.9835E-07	0.0942
	1.9071E-07	0.0905
	0.0000E+00	0.0000
	2.7081E-08	0.0129
	0.0000E+00	0.0000

5.3.4 PZR Safety Nozzle C Axial Final Flaw Size Evaluation

As seen in Section 5.3.3, there is virtually no flaw growth. Table 5-15 shows evaluation of the final flaw size with the flaw acceptance standard of Appendix C of the ASME B&PV Code Section XI [2]. It is seen from Table 5-15 that the final flaw size is much smaller than the allowable flaw size. Therefore, the indications found in PZR Safety Nozzle C are acceptable for the remainder of the plants service life.

Table 5-15: PZR Safety Nozzle C Axial Final Flaw Size Evaluation

Allowable Flaw Depths	Normal	Upset	Faulted	Reference [2]
Service level maximum pressure, p, (psi)	[ ]	[ ]	[ ]	
Service level maximum temperature, T, (F)	[ ]	[ ]	[ ]	
Service level flow stress, $\sigma_f = (Sy+Su)/2$, (psi)	[ ]	[ ]	[ ]	
Total thickness, t , (inch)	[ ]	[ ]	[ ]	
Overlay outside diameter, Do, (inch)	[ ]	[ ]	[ ]	
Inside diameter, Di, (inch)	[ ]	[ ]	[ ]	
Mean pipe radius, Rm (inch)	[ ]	[ ]	[ ]	
Final Flaw Depth, a_f , (in)	0.210	0.210	0.210	
Final flaw length, l_f (inch)	0.250	0.250	0.250	
Nondimensional flaw length, $l_f / (R_m t)^{0.5}$	[ ]	[ ]	[ ]	C-5410
Pipe hoop stress, $\sigma_h = pR_m/t$, (psi)	[ ]	[ ]	[ ]	C-5410
Stress ratio, σ_h / σ_f	[ ]	[ ]	[ ]	C-5410
Allowable flaw depth to thickness ratio, a_{allow}/t,	0.75	0.75	0.75	Table 5410-1
Final flaw depth to thickness ratio, a_f / t,	0.1440	0.1440	0.1440	

$l_f = (a_f / ai) * l_i$

5.4 PZR Spray Nozzle NDE Occlusion Zone

5.4.1 PZR Spray Nozzle Circumferential Flaw Growth Analysis

The calculated flaw growth for the postulated circumferential flaw (representing NDE occlusion region) in PZR Spray Nozzle is small. Table 5-16 shows a summary of the crack growth as calculated by AREVACGC. Table 5-17 shows the contribution of each analyzed transient to the calculated fatigue crack growth.

Table 5-16: PZR Spray Nozzle Circumferential Flaw Growth - Summary

Initial Flaw Depth (in) =	0.5520
Initial a/t ratio =	0.5923
Final Flaw Depth (in) =	0.5526
Final a/t ratio =	0.5929
Total Amount of Fatigue Crack Growth (in) =	5.6910E-04

Table 5-17: PZR Spray Nozzle Circumferential Flaw Growth – Detailed Analysis

Trans.	Growth (in)	Percent
	2.6470E-05	4.6512
	4.8068E-06	0.8446
	1.7591E-04	30.9103
	1.7539E-04	30.8195
	9.2776E-05	16.3023
	9.2675E-05	16.2846
	0.0000E+00	0.0000
	0.0000E+00	0.0000
	0.0000E+00	0.0000
	0.0000E+00	0.0000
	0.0000E+00	0.0000
	0.0000E+00	0.0000
	0.0000E+00	0.0000
	0.0000E+00	0.0000
	0.0000E+00	0.0000
	1.0665E-06	0.1874
	0.0000E+00	0.0000
	0.0000E+00	0.0000

5.4.2 PZR Spray Nozzle Circumferential Final Flaw Size Evaluation

As seen in Section 5.4.1, the crack growth for the postulated circumferential flaw is small. Table 5-18 shows evaluation of the final flaw size with the flaw acceptance standard of Appendix C of the ASME B&PV Code Section XI [2]. It is seen from Table 5-18 that the final flaw size is smaller than the allowable flaw size. Therefore, the indications found in PZR Spray Nozzle are acceptable for the remainder of the plants service life.

Table 5-18: PZR Spray Nozzle Circumferential Final Flaw Size Evaluation

Allowable Flaw Depths	Normal	Upset	Faulted	Reference [2]
Service level maximum pressure, p, (psi)	[ ]	[ ]	[ ]	
Service level maximum temperature, T, (F)	[ ]	[ ]	[ ]	
Service level flow stress, $\sigma_f = (Sy+Su)/2$, (psi)	[ ]	[ ]	[ ]	
Total thickness, t , (inch)	[ ]	[ ]	[ ]	
Overlay outside diameter, D_o, (inch)	[ ]	[ ]	[ ]	
Sectional area, A, (inch^2)	[ ]	[ ]	[ ]	
Moment of inertia, I, (inch^4)	[ ]	[ ]	[ ]	
Section modulus, S (inch3)	[ ]	[ ]	[ ]	
Primary Bending Moment, $M_{b\ SRSS}$ (in-lbf)	[ ]	[ ]	[ ]	
Thermal Expansion Bending Moment, $M_{e\ SRSS}$ (in-lbf)	[ ]	[ ]	[ ]	
Safety factor, SFm,	2.7	2.4	1.3	C-2621
Safety factor, SFb,	2.3	2.0	1.4	C-2621
Calculated primary membrane stress, $\sigma_m = pD_o/4t$, (psi)	[ ]	[ ]	[ ]	C-2500
Calculated primary bending stress, σ_b = Moment SRSS/S , (psi)	[ ]	[ ]	[ ]	C-2500
Calculated secondary bending stress, σ_e = Moment SRSS/S, (psi)	[ ]	[ ]	[ ]	C-2500
Final Flaw Depth, a_f , (in)	0.553	0.553	0.553	
Final Flaw length, l_f , (in)	16.824	16.824	16.824	
Calculated final flaw depth to thickness ratio, a_f /t,	[ ]	[ ]	[ ]	
Stress ratio, $[\sigma_m + \sigma_b] / \sigma_f$	[ ]	[ ]	[ ]	C-5311
Ratio of flaw length to pipe circumference, $l_f / \pi D_o$,	[ ]	[ ]	[ ]	C-5311
Ratio of allowable flaw depth to thickness, a_{allow} / t,	0.750	0.750	0.750	Table C-5310-1,2,4
Allowable flaw depth, a_{allow} , (in)	0.699	0.699	0.699	

5.4.3 Spray Nozzle Axial Flaw Growth Analysis

The calculated crack growth for postulated axial flaw (representing NDE occlusion region) in PZR Spray Nozzle is small. Table 5-19 shows a summary of the crack growth as calculated by AREVACGC. Table 5-20 shows the contribution of each analyzed transients to the calculated fatigue crack growth.

Table 5-19: Spray Nozzle Axial Flaw Growth - Summary

Initial Flaw Depth (in) =	0.5520
Initial a/t ratio =	0.5923
Final Flaw Depth (in) =	0.5645
Final a/t ratio =	0.6057
Total Amount of Fatigue Crack Growth (in) =	1.2527E-02

Table 5-20: Spray Nozzle Axial Flaw Growth – Detailed Analysis

Trans.	Growth (in)	Percent
	2.6560E-04	2.1203
	3.5134E-04	2.8046
	5.2481E-04	4.1895
	5.2041E-04	4.1544
	9.2847E-05	0.7412
	9.1917E-05	0.7338
	5.9120E-03	47.1946
	9.1967E-06	0.0734
	4.1169E-05	0.3286
	4.1701E-05	0.3329
	4.6470E-03	37.0962
	1.1095E-05	0.0886
	4.6323E-06	0.0370
	0.0000E+00	0.0000
	6.3709E-06	0.0509
	6.7911E-06	0.0542
	0.0000E+00	0.0000

5.4.4 Spray Nozzle Axial Final Flaw Size Evaluation

As seen in Section 5.4.3, there is virtually small flaw growth for the postulated axial flaw. Table 5-21 shows evaluation of the final flaw depth with flaw acceptance standard from Appendix C of the ASME B&PV Code Section XI. It is seen from Table 5-21 that the final flaw size is much smaller than the allowable flaw size. Therefore, the indications found in PZR Safety Nozzle B are acceptable for the remainder of the plants service life.

Table 5-21: Spray Nozzle Axial Final Flaw Size Evaluation

Allowable Flaw Depths	Normal	Upset	Faulted	Reference [2]
Service level maximum pressure, p, (psi)	[ ]	[ ]	[ ]	
Service level maximum temperature, T, (F)	[ ]	[ ]	[ ]	
Service level flow stress, $\sigma_f = (Sy+Su)/2$, (psi)	[ ]	[ ]	[ ]	
Total thickness, t , (inch)	[ ]	[ ]	[ ]	
Overlay outside diameter, Do, (inch)	[ ]	[ ]	[ ]	
Inside diameter, Di, (inch)	[ ]	[ ]	[ ]	
Mean pipe radius, Rm (inch)	[ ]	[ ]	[ ]	
Final Flaw Depth, a_f , (in)	0.565	0.565	0.565	
Final flaw length, l_f (inch)	1.129	1.129	1.129	
Nondimensional flaw length, $l_f / (R_m t)^{0.5}$	[ ]	[ ]	[ ]	C-5410
Pipe hoop stress, $\sigma_h = pR_m/t$, (psi)	[ ]	[ ]	[ ]	C-5410
Stress ratio, σ_h / σ_f	[ ]	[ ]	[ ]	C-5410
Allowable flaw depth to thickness ratio, a_{allow}/t,	0.75	0.75	0.75	Table 5410-1
Final flaw depth to thickness ratio, a_f / t,	0.61	0.61	0.61	

6.0 SUMMARY AND CONCLUSION

This document performed flaw evaluations for indications found in DCPP Unit 2 PZR Safety Nozzles A, and NDE occlusion zones in PZR Safety Nozzles B and C and PZR Spray Nozzle. The conclusion of the flaw evaluations shows that the indications in PZR Safety Nozzle A and NDE occlusion zones in PZR Safety Nozzle B and C and PZR Spray Nozzle meet the flaw acceptance standards of ASME B&PV Code Section XI, IWB-3514. All indications and postulated flaws in the NDE occlusion zones for all nozzles meet the ASME B&PV Code Section XI, IWB-3640.

7.0 REFERENCES

1. AREVA Document 38-9200149-000, (DCPP Unit 2 DIT-50540188-03-00), "DCPP Unit 2 Pressurizer Nozzle NDE Data."
2. ASME Boiler and Pressure Vessel Code, Section XI, "Rules for Inservice Inspection of Nuclear Power Plant Components", 2004 Edition with Addenda through 2005.
3. AREVA Document 32-9199937-000, "DCPP Unit 2 Evaluation of Laminar Indications on Pressurizer Nozzles".
4. AREVA Document 32-9043545-001, "Diablo Canyon Unit 2, Pressurizer Safety/Relief Nozzle Weld Overlay Sizing Calculation."
5. AREVA Document 32-9043546-001, "Diablo Canyon Unit 2, Pressurizer Spray Nozzle Weld Overlay Sizing Calculation."
6. AREVA Document 32-9049114-001, "Diablo Canyon Unit 2 Pressurizer Safety/Relief Nozzle Weld Overlay Analysis."
7. AREVA Document 32-9049062-002, "Diablo Canyon Unit 2 Pressurizer Safety/Relief Nozzle Weld Overlay Residual Stress Analysis."
8. Diablo Canyon Unit 2 ASME Section XI Inservice Inspection Program Relief Request REP-1 U2, Docket No. 50-323, OL-DPR-82, ML070990060.
9. AREVA Document 32-9049065-001, "The Diablo Canyon Unit 2 pressurizer Safety/Relief Nozzle Weld Overlay Crack Growth Evaluation."
10. AREVA Document 32-9049064-001, "Diablo Canyon Unit 2 PZR Spray Nozzle Weld Overlay Crack Growth Evaluation."
11. AREVA Drawing 02-8019311D-001, "Diablo Canyon Pressurizer Safety & Relief Nozzle Weld Overlay Design Input."
12. AREVA Drawing 02-8018401C-001, "Diablo Canyon Unit 2 Pressurizer Safety/Relief Nozzle Existing Configuration."
13. AREVA Drawing 02-8018400C-002, "Diablo Canyon Unit 2 Pressurizer Spray Nozzle Existing Configuration."
14. AREVA Drawing 02-8019233D-001, "Diablo Canyon Pressurizer Spray Nozzle Weld Overlay Design Input."
15. AREVA Document 32-9055891-006, "Fatigue and PWSCC Crack Growth Evaluation Tool AREVACGC."
16. AREVA Document 32- 9052958-003, "Evaluation of stress intensity factors using the weight function method."
17. AREVA Document 32-9049061-003, "Diablo Canyon Unit 2 PZR Spray Nozzle Weld Overlay Residual Stress Analysis."
18. AREVA Document 38-9046469-002, "Design Input Transmittal – Diablo Canyon 2."
19. AREVA Document 32-9049112-001, "Pressurizer Spray Nozzle Weld Overlay Structural Analysis."
20. NUREG/CR-6721, "Effects of Alloy Chemistry, Cold Work, and Water Chemistry on Corrosion Fatigue and Stress Corrosion Cracking of Nickel Alloys and Welds," U.S. Nuclear Regulatory Commission (Argonne National Laboratory), April 2001.

21. NRC Letter from Richard Barrett, Director Division of Engineering, Office of NRR to Alex Marion of Nuclear Energy Institute, "Flaw Evaluation Guidelines," April 11, 2003, Accession Number ML030980322.

22. Enclosure 2 to Reference [21], "Appendix A: Evaluation of Flaws in PWR Reactor Vessel Upper Head Penetration Nozzles," Accession Number ML030980333.